AN ABSTRACT OF THE THESIS OF

Brijesh Singla for the degree of Master of Science in Chemical Engineering presented on February 16, 1995. Title: Adsorption of Synthetic Stability Mutants of Bacteriophage T4 Lysozyme at Silanized Silica Surfaces.

Redacted for Privacy

Abstract approved: _____

Dr. Joseph McGuire

The adsorption kinetics exhibited by the wild type and two synthetic stability mutants of bacteriophage T4 lysozyme at silanized silica surfaces were monitored with *in situ* ellipsometry. Mutant lysozymes purified from *Escherichia coli* strain RRI were produced by substitution of the isoleucine at amino acid position three with cysteine, and tryptophan, yielding a set of proteins with values of $\Delta G_{unfolding}$ ranging from 1.2 kcal/mol greater to 2.8 kcal/mol less than that of the wild type. The adsorption kinetics of the wild type protein and each mutant were measured at hydrophobic and hydrophilic silica surfaces and interpreted with reference to two kinetic models. One was a three-rate-constant model allowing for reversible, initial binding followed by conversion to an irreversibly adsorbed form, whereas the second model allowed for irreversible adsorption into one of two states directly from solution. State 1 molecules were defined as being less tightly bound and occupying less interfacial area than those in state 2. Substantial differences in adsorption kinetic behavior were observed among the proteins. In particular, each model suggested that a protein of lower structural stability more readily undergoes a

surface-induced structural change, all other things being equal, and this change was more pronounced on hydrophilic than on hydrophobic surfaces.

Adsorption of Synthetic Stability Mutants of Bacteriophage T4 Lysozyme at Silanized Silica Surfaces

by

Brijesh Singla

A THESIS

submitted to

Oregon State University

in partial fulfillment of
the requirements for the
degree of

Master of Science

Completed February 16, 1995
Commencement June, 1995

Master of Science thesis of Brijesh Singla presented on February 16, 1995

APPROVED:

Redacted for Privacy

Major Professor, representing Chemical Engineering

Redacted for Privacy

Head of Department of Chemical Engineering

Redacted for Privacy

Dean of Graduate School

I understand that my thesis will become part of the permanent collection of Oregon State University libraries. My signature below authorizes release of my thesis to any reader on request.

Redacted for Privacy

Brijesh Singla, Author

ACKNOWLEDGMENT

I wish to express my gratitude to Dr. Joseph McGuire, my major professor, for his valuable support and guidance. I would like to thank Dr. Michael H. Penner, Dr. Goran Jovanovic, and Dr. Edward H. Piepmeier for kindly serving as my committee members.

My appreciation is also extended to Dr. Viwat Krisdhasima and my co-worker, Nilobon Podhipleux for their help and timely suggestions. Special thanks to Professor Brian Matthews and Sheila Snow of the Institute of Molecular Biology, University of Oregon, for providing bacterial strains required for this research.

I would also like to acknowledge the constant moral support and encouragement of my family members and my girl-friend, Nidhi.

This work was mainly supported by National Science Foundation, and in part by the Medical Research Foundation of Oregon, and the Whitaker Foundation.

TABLE OF CONTENTS

LIST OF FIGURES

LIST OF TABLES

LIST OF APPENDICES

NOMENCLATURE

A_1 = Interfacial area occupied by state 1 molecules, cm^2

A_2 = Interfacial area occupied by state 2 molecules, cm^2

a = Ratio of area occupied by state 2 molecules and that of state 1 molecules.

C = Protein concentration, mg/mL

$\Delta\Delta G$ = The difference between the free energy of unfolding of the mutant and that of the wild type at the melting temperature of the wild type

k_1 = Adsorption rate constant, mL/mg-min, in equation [1]

k_{-1} = Desorption rate constant, min^{-1}

k_1 = Rate constant for adsorption in state 1, mL/mg-min, in equation [14]

k_2 = Rate constant for adsorption in state 2, mL/mg-min, in equation [15]

k_s = Rate constant for surfactant-mediated removal of protein, min^{-1}

s_1 = Conformational change rate constant, min^{-1}

t = Time, min

t_i = Time at which protein in contacted with pure buffer, min

t_s = Time of surfactant addition, min

Γ = Adsorbed mass, $\mu g/cm^2$

Γ_{max} = Maximum mass of molecule that could be adsorbed in a monolayer, $\mu g/cm^2$

θ_1 = Fractional surface coverage of reversible adsorbed protein in equation [1]

θ_2 = Fractional surface coverage of irreversible adsorbed protein in equation [2]

θ_1 = Mass of molecules adsorbed ($\mu g/cm^2$) in state 1, divided by Γ_{max} ($\mu g/cm^2$) in equation [14]

θ_2 = Mass of molecules adsorbed ($\mu g/cm^2$) in state 2, divided by Γ_{max} ($\mu g/cm^2$) in equation [15]

λ = Wavelength, nm

Δ = The change in phase of light, degrees

ψ = The arctangent of the factor by which the amplitude ratio changes

ADSORPTION OF SYNTHETIC STABILITY MUTANTS OF BACTERIOPHAGE T4 LYSOZYME AT SILANIZED SILICA SURFACES

1. INTRODUCTION

The interfacial behavior of proteins has been the topic of significant discussion regarding many technological and biological areas, such as biomaterials, food processing, chromatography, pharmaceutics and biomembranes. Protein adsorption occurs when its solution is brought in contact with a foreign material. It is a phenomenon involving the attachment of different amino acid residues to the sorbent surface, and interfacial properties are altered as a consequence.

In most biological fluids such as blood and milk, proteins can interact with any surface they encounter resulting in their adsorption. Membrane filtration is used extensively in milk processing, and it is known that fouling can reduce the flux through the membrane by about 90% compared to that of pure water (1). The behavior of blood serum proteins at the site of implantation of a foreign device is related to the biocompatibility of the device. Protein separation and purification by chromatographic means requires a thorough understanding of protein behavior at specific interfaces. Adsorption at chromatographic supports involves interactions with the protein molecules through hydrophobic, ion exchange, or charge transfer mechanisms. A study of molecular mechanisms influencing a protein's adsorption at interfaces is of great importance in the development of new biosensors and bioseparation technology.

There is much known in a quantitative sense about the nature of an adsorbed layer (2,3), but predictive models to describe the various aspects of protein adsorption as a function of protein and interfacial properties are lacking. The complexity in predicting its behavior at the interfaces arises from the fact that amino acid residues exhibiting their polar/nonpolar, cationic/anionic, and hydrophobic/hydrophilic character are non-uniformly distributed, and hence cause an overall geometric asymmetry in the molecules. One approach to better understand the molecular basis of protein adsorption is to study sets of very similar proteins differing only in some controlled property, e.g., a set of proteins differing in structural stability, but that are otherwise virtually identical.

Recent progress in recombinant DNA techniques, especially site-directed mutagenesis, has made it possible to modify protein structure almost at will. The objective of this research was to study structural stability influences on adsorption by using two synthetic stability mutants of bacteriophage T4 lysozyme, in which the isoleucine residue at position three was replaced with cysteine, and with tryptophan, by site-directed mutagenesis. The adsorption kinetics of the wild type protein and each mutant were measured at silanized hydrophobic and hydrophilic silica surfaces and interpreted with reference to two kinetic models.

In this way we will start comparing kinetic rate constants for protein adsorption and rearrangement to intrinsic properties of the molecules, in this case thermostability, quantified by $\Delta\Delta G$: the difference between the free energy of unfolding of the mutant and that of the wild type at the melting temperature of the wild type. Substantial evidence exists indicating that for simple single domain proteins the thermostability in solution

would correlate with its interfacial behavior. Some of this evidence is presented in the next section.

2. LITERATURE REVIEW

2.1 Protein Adsorption and its Significance

Proteins are biological macromolecules synthesized in the cell for unique functions. They are high molecular weight polyamides produced by the copolymerization of up to 20 different amino acids. Amino acid composition constituting primary structure is generally specific to each protein. The backbone of proteins form various secondary structures, such as α-helix and β-sheet. Intramolecular association, e.g., ionic interactions, salt bridges, hydrophobic interactions, hydrogen bonding, and covalent disulfide bonds, contribute a tertiary structure for each polypeptide chain. Finally, two or more polypeptide chains, each with its own primary, secondary, and tertiary structure, can associate to form a multi-chain quaternary structure (2). If the protein is adsorbed such that its three-dimensional shape or secondary structure changes, then the protein is said to undergo a change of conformation. A conformational change is often termed as "denaturation" or "unfolding".

Mechanisms of protein adsorption on solid surfaces are very complicated not only by the size and complexity of macromolecules but also by the necessity to account for very small energy changes in both the folded and the unfolded forms. The net difference between the free energies of the folded and unfolded forms is as small as 5-20 kcal/mol. A change in energy of a few kilocalories per mole in either the folded or the unfolded form of a protein can substantially alter its stability and structure (3). The protein-surface interactions, in addition to the diffusion of protein molecules to the solid surface, contain a large number of time-dependent variables. Time dependency may be involved in a) the

development of the bonds between the surface and the protein molecules, b) the lateral mobility of the molecules, and c) the conformational changes of the molecules occurring due to the interactions between the surface and the molecules. Figure 1 summarizes the basic components of the protein adsorption process. Protein adsorption is often an apparently irreversible phenomena, i.e., the amount of organic matter on the surface remains constant when the solution around the surface is depleted of protein.

2.2 Structural Stability of Proteins at Interfaces

Comparative studies of protein interfacial behavior have made it possible to begin to measure the influence of molecular properties, on protein adsorption affinity by studying similar proteins (4-6), genetic variants (7,8) or site-directed mutants of a single protein (9). There are a number of factors that affect protein surface activity, but protein stability has drawn a lot of attention out of charge, surface hydrophobicity and solution properties in many of the past studies. The importance of structural stability in protein interfacial behavior has been demonstrated by studying, genetic variants and site-directed mutants of single proteins.

Asakura et al. (10) reported that the oxy-form of abnormal hemoglobin (hemoglobin S), predominant in the red cells of humans with the sickle cell disease, precipitated from its solution very quickly when shaken, unlike solutions of the normal hemoglobin A variant, and attributed this phenomenon to greater surface-induced denaturation upon exposure of hemoglobin S molecules to the gas-liquid interface, relative to that experienced by hemoglobin A. Their finding that the abnormal hemoglobin

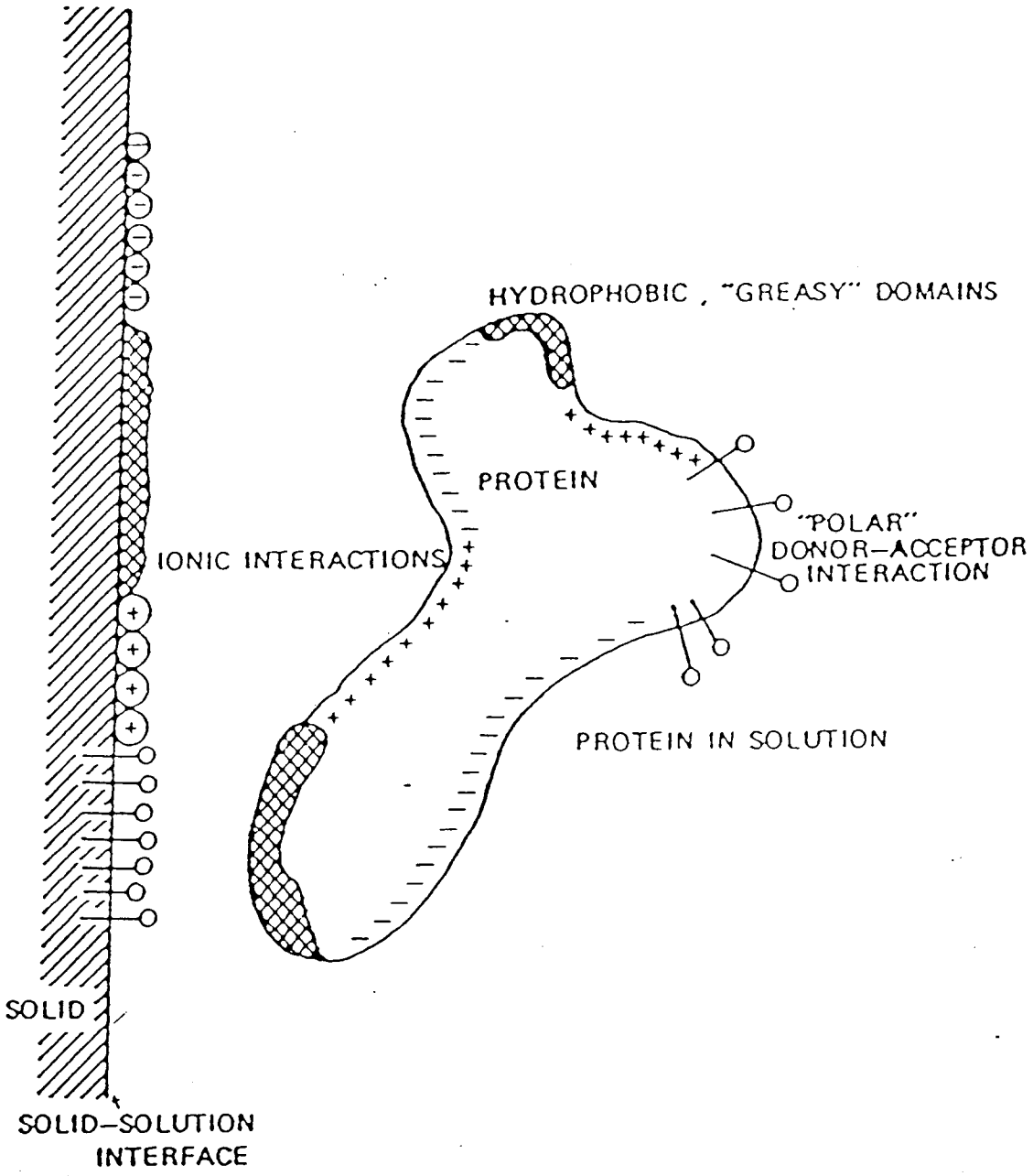

Figure 1. A schematic view of a protein interacting with a well-characterized surface (2)

denatured more rapidly during stirring in the absence of bubbles led them to conclude that although believed to be similar, the conformation of the oxy-form of hemoglobin S in solution was likely less stable than that of hemoglobin A (10,11). These studies set up the basis for studying interfacial behavior of several single-point mutants of human hemoglobin, with reference to structural changes and the relationship between interfacial behavior and stability during mechanical treatment. Mutants containing the glutamic acid →valine substitution at the sixth position in the β-chains, characteristic of hemoglobin S, were found to exhibit faster kinetics and greater spreading pressure at apparent equilibrium than did hemoglobin A, and hence the possible importance of differences in protein unfolding and spreading at the air-water interface was emphasized. They concluded that differences between the mechanical stability of oxy-forms of hemoglobin A and hemoglobin S were mainly due to differences in their interfacial behavior.

Horsley et al. (7) made a comparison of isotherms constructed for hen and human lysozyme at silica derivitized negatively-charged, positively-charged, or hydrophobic surfaces. These workers explained some of the differences in adsorptive behavior of the two lysozyme variants by knowing that human lysozyme contains one less disulfide bond, and is of lower thermal stability than hen lysozyme, and by visualization with molecular graphics. They attributed the reason of human lysozyme displaying much larger changes in the denaturation parameters upon adsorption than those for hen lysozyme to its less conformational stability at different types of interfaces. Xu and Damodaran (12) compared adsorption kinetic data measured for native and denatured hen, human, and bacteriophage T4 lysozymes at the air-water interface. The differences in adsorption dynamics among

these three variants were attributed to the chemical potential gradient arising due to interactions between the interfacial force field and various molecular potentials (conformational or entropic, hydrophobic, electrostatic, and hydration), rather than concentration gradient alone.

Kato and Yutani (8) measured the surface properties of wild-type and six mutant α-subunits of tryptophan synthase substituted at the same position, 49, in the protein interior, by correlating surface tension, foaming and emulsifying properties with their structural stabilities. The conformational stabilities of these subunits, as measured by their free energy of denaturation in water (ΔG_{water}), varied from 5-17 kcal/mol, depending on the characteristics of the substituting residue into position 49. They attributed differences in interfacial behavior of these proteins to their Gibbs free energy of unfolding in water, and observed that more stable mutant proteins, substituted by isoleucine and phenylalanine in place of glutamic acid at position 49, exhibit greater resistance to unfolding and orientation at the interface.

Krisdhasima et al. (13) studied surface induced conformational changes in milk proteins α-lactalbumin (α-lac), β-lactoglobulin (β-lag), and bovine serum albumin (BSA). They attributed the differences in the surface activities of these molecularly dissimilar globular proteins to their relative flexibility, molecular size and stability, and hence concluded that the proteins with lower structural stability/or higher flexibility are preferentially adsorbed. These workers recorded adsorption kinetic data, along with surface-mediated elutability of each protein with reference to a simple kinetic model for protein adsorption. The model included an initial, reversible adsorption step, followed by a

surface-induced conformational change yielding an irreversibly form of protein molecules. The relative magnitudes of rate constants defining arrival and unfolding were found to be consistent with molecular properties influencing surface activity of each protein.

McGuire et al. (14) measured the effect of structural stability on adsorption and dodecyltrimethylammonium bromide (DTAB)-mediated elutability of synthetic mutants of bacteriophage T4 lysozyme at silica derivitized surfaces, and attributed the differences in interfacial behavior among the proteins with respect to both the adsorption kinetic behavior and the DTAB-mediated elutability, to protein stability. They concluded that less stable proteins more readily make the conversion from removable to a nonremovable form.

Billsten et al. (15) studied the change in secondary structure of T4 lysozyme upon adsorption to silica particles by circular dichroism (CD). The mutants different from wild type by substitution of isoleucine for cysteine and tryptophan were investigated. They concluded that CD spectra of Ile3→Trp adsorbed from aqueous solution onto dispersed silica particles show great structural changes relative to the CD spectra for either wild type or Ile3→Cys(S-S) adsorbed to the same surface, while their solution spectra is similar.

2.3 Bacteriophage T4 Lysozyme

Bacteriophage T4 lysozyme was the protein of choice in this work for several reasons. It has been well characterized biochemically and mutants enzymes can be obtained which differ from the wild type enzyme in stability. Its three-dimensional structure and surface morphology are well known. The α-carbon backbone of T4 lysozyme is shown in Figure 2. It is a basic molecule with isoelectric point above 9.0 and

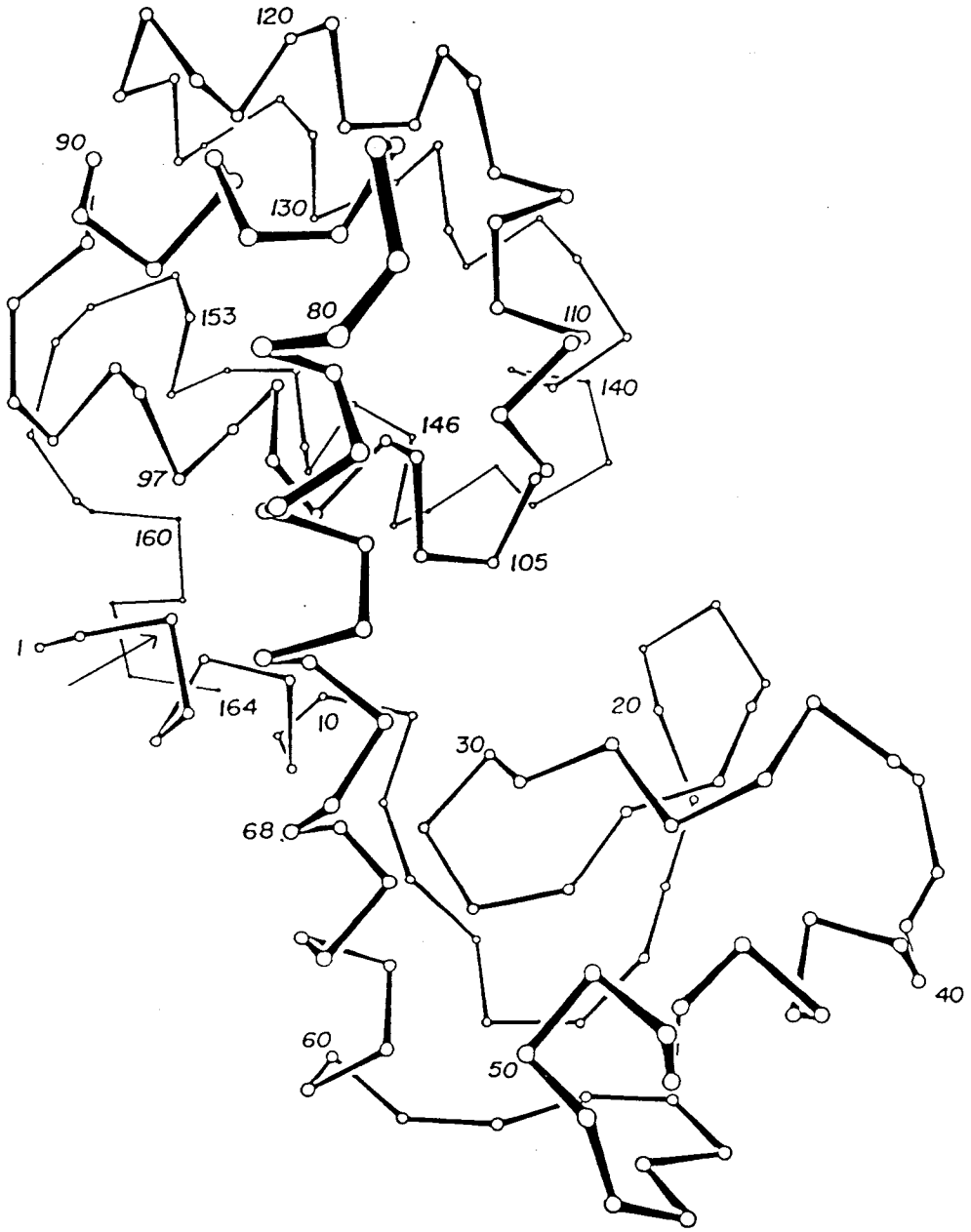

Figure 2. The α-carbon backbone of the wild type lysozyme from bacteriophage T4.

an excess of nine positive charges at neutral pH. T4 lysozyme has 164 amino acids residues and a molecular weight of about 18,700 daltons (16).

Functions and properties: The function of the enzyme is to hydrolyze the glycosidic linkages in the bacterial cell wall resulting in cell lysis. Phage lysozyme is similar to hen egg-white lysozyme in that both enzymes cleave the same glycosidic bond, but T4 lysozyme is 250-fold more active towards *E. coli* cell walls (17). Because it resembles egg-white lysozyme in certain aspects, it has been named phage lysozyme (18), however, the amino acid sequence of each lysozyme has been found to be nonhomologous. This enzyme is also contained in mature phage particles (19); lysates of bacteriophage T4 contain an enzyme that digests cell walls of *E. coli*.

T4 lysozyme has twenty eight positively charged groups (17,20) out of which there are thirteen arginine, thirteen lysine, one histidine and the terminal amino group, and ten asparagine, eight glutamine and the terminal carboxylate group constitute eighteen negatively charged groups (21). It is clear from Figure 2 that the molecule has two distinct domains: the C-terminal and N-terminal lobes, joined by an α-helix (residues 60-80). Most of the excess positive charges reside on the C-terminal lobe (22), while the charge on the N-terminal lobe is relatively balanced. Most of the negative charges interact either with positively charged side chains or with helix dipole charges, or are involved in hydrogen-bonding interactions (23), but only eighteen positively charged residues are involved in such interactions. The remaining ten do not have any groups for hydrogen bonding within a distance of 3.5 Å. The side chains of these ten charged residues, including the amino terminus, are well exposed to the solvent and are very mobile (20,24). The two domain

structure of the enzyme is more distinct than for hen lysozyme, although similarities exist at the tertiary level. There is no disulfide linkage (20) in T4 lysozyme, and crystallographic data show T4 lysozyme as an ellipsoid of about 54 Å long, with the diameter of C and N-terminal lobes about 24 Å and 28 Å, respectively (16,25,26).

Isoleucine at position three (Ile 3) of bacteriophage T4 lysozyme has been replaced with thirteen different amino-acid residues by site-directed mutagenesis and resulting variants are characterized with respect to their deviations from the wild type in crystal structure and thermodynamic stability (27). Overall, structures of these proteins have been shown to be similar to wild type.

The contribution of hydrophobic interaction at the site of Ile 3 to the overall stability of the protein has been quantified (27) by $\Delta\Delta G$: the difference between the free energy of unfolding of the mutant and that of the wild type at the melting temperature of the wild type (21). In wild type lysozyme, Ile 3 contributes to the major hydrophobic core of the C-terminal lobe and also helps link the N and C-terminal domains. The side chain of Ile 3 is 80% inaccessible to solvent and contacts the side chains of methionine at position 6, leucine at position 7, and isoleucine at position 100; it also contacts the main chain of cysteine at position 97. These four residues are buried within the protein interior (27).

3. MATERIALS AND METHODS

3.1 Protein Purification

Synthetic stability mutants of T4 lysozyme were produced from transformed cultures of bacterium strain RRI. Individual bacterium strains, containing the mutant lysozyme expression vectors desired for the present work, were provided by Professor Brian Matthews and co-workers at the Institute of Molecular Biology, University of Oregon, Eugene, OR. Expression and purification of the mutants was carried out, from this point onward, following established procedures (21,28,29). The cells bearing the desired mutant lysozyme expression vector, which carries an ampicillin resistant gene, were grown overnight in an incubator at 37°C for 8 to 9 h in 100 mL of LB-H broth (Appendix A) with 10 mg ampicillin. This culture was then added to a 7-liter autoclaved fermenter containing 4.8 liters of LB broth (Appendix A), 400 mg ampicillin and 1.5 mL tributyl phosphate as anti-foam agent, for further growth at 35°C until the optical density (checked by DU® Series 60 Spectrophotometer, Beckman Instruments, Inc. Fullerton, CA) at 595 nm near about 0.8 (about 2 hours). The impeller speed was adjusted at 600 rpm and the air inflow, after filtering through prefilter and filter (millipore 45 mm), at 12-14 L/min. At this point the temperature was lowered to 30°C and 750 mg IPTG (isopropyl-β-thiogalactoside) was added to the growth media to induce lysozyme expression. The fermentation was further continued at 200 rpm, 7-8 L/min air inflow for 110 min. The cells were then harvested and centrifuged, first at 1.2K rpm in F16/250 rotor (Sorvell RC28S, Du Pont Medical Products, Hoffman Estate, IL) for 20 min, and then at

12.5K rpm for 30 min. From this point, all the purification procedures were carried out at 4°C.

Mutant proteins were purified from both the pellet and supernatant fractions. The pellet from the prior centrifugation were resuspended with 20 mL of 10 mM Tris buffer, pH 7.4. Lysis buffer (0.10 M sodium phosphate, 0.2 M NaCl, 10 mM $MgCl_2$, pH 6.6) was added to a final volume of 200 mL. 1 mL of 0.5 M EDTA, pH 8.0, was added to each 100 mL of resuspended cells. The suspension was stirred for about 12 h, and then 10 mg of DNase 1 (Deoxyribonuclease) together with 1 mL of 1 M $MgCl_2$ per 100 mL were added to the suspension to degrade chromosomal DNA. The suspension was stirred for 2 h at room temperature to promote cell lysis. It was then centrifuged at 20K in F28/50 rotor for 30 min, the pellet discarded, and the supernatant was combined with that from previous centrifugation. Each 1100 mL of this total supernatant was dialyzed against deionized, distilled water until its conductivity was between 2 and 3 μmho/cm. Its pH was then adjusted to neutrality (between 6.5 and 7.5) and the solution loaded onto a 2.5 X 7 cm CM - Cepharose (CCL - 100) ion exchange column, which was previously equilibrated with 50 mM Tris buffer, pH 7.25. A salt gradient from 0.05 M to 0.30 M NaCl in 50 mM Tris was used to elute the column into a fraction collector (Frac-100, Pharmacia LKB Biotechnology, Alameda, CA). The elution was monitored with a UV monitor (Optical unit UV-1 and control unit UV-1, Pharmacia LKB Biotechnology), and output was recorded on a chart recorder. Eluted fractions having O.D. > 0.7 at 280 nm were collected in Spectra/Por molecular porous membrane tubing (10,000-14,000 molecular weight cutoff, Spectrum Medical Industries, Inc.) and dialyzed against 50 mM sodium phosphate

buffer, 20 times the elution volume, pH 5.8, containing 0.02% sodium azide (NaN_3) for about 12 h and then concentrated by loading onto 1 X 2 cm SP Sephadex column (C-50).

Mutant proteins were eluted with 0.10 M sodium phosphate, pH 6.5, containing 0.55 M NaCl and 0.02% NaN_3. The yield of lysozymes was usually between 40-100 mg, with total volume of 2-4 mL, and were stored at 4°C without further treatment. The mutant lysozymes were determined by Sodium dodecylsulfate polyacrylamide electrophoresis (SDS-PAGE) to be over 95% pure. The remaining fractions of less then 5% contain salts and unknown peptide fragments, and there is no evidence that they influence any of the trends observed in the experiments.

In addition to the wild type lysozyme, two stability mutants were purified for study. A mutant with cysteine substituted for Ile 3 (Ile 3→Cys(S-S)) was selected, within which a disulfide link is formed with Cys 97, to give a more stable protein than the wild type ($\Delta\Delta G$ = +1.2 kcal/mol at pH 6.5). A mutant with tryptophan substituted for Ile 3 (Ile 3 →Trp) was selected as it is one of the least stable lysozymes synthesized to date ($\Delta\Delta G$ = -2.8 kcal/mol at pH 6.5).

3.2 Protein Solution Preparation

Lysozyme stored in vials at 4°C were diluted with phosphate buffer, pH 7.0 to obtain a protein solution of concentration equivalent to 1 mg/mL of β-lactoglobulin. Buffer solution constituted 0.01M sodium phosphate monobasic monohydrate ($NaH_2PO_4.H_2O$), 0.01M sodium phosphate dibasic (NaH_2PO_4), and 0.02% (mass/volume) of sodium azide (NaN_3) as anti-microbial agent, and it was filtered (0.22 mm type GV,

Millipore Corp., Bedford, MA) before using it for diluting protein. All protein concentrations used throughout this work are expressed as equimolar concentration of β-lactoglobulin.

3.3 Surface Preparation

All surfaces were prepared from single type of silicon (Si) wafer (hyperpure, type N, phosphorus doped, orientation 1-0-0; Wacker Siltronic Corp., Portland, OR). First, the Si wafers were cut into small plates of approximately 1 X 2 cm using a tungsten pen. They were subsequently treated to exhibit hydrophobic or hydrophilic surfaces by silanization with dichlorodimethylsilane (DDS, Aldrich Chemical Co., Inc., Milwaukee, WI) according to the procedure of Jöhnson et al. (30), as slightly modified by Wahlgren and Arnebrant (31). Each small Si plate was placed into a test tube and 5 mL of the mixture $NH_4OH/H_2O_2/H_2O$ (1/1/5) was added to the tube followed by heating to 80°C in a water bath for 15 min. The plates were then rinsed with 20 mL of deionized, distilled water (Corning Megapure System, Corning, N.Y.) before immersing in 5 mL HCl/ H_2O_2/H_2O (1/1/5) for 15 min. at 80°C. Each plate was again rinsed with 30 mL deionized, distilled water and stored in 20 mL of 50% ethanol-water solution to maintain stability until further use.

Surfaces were stored in a desiccator for 24 h after rinsing with deionized, distilled water and drying with N_2. The surfaces were made hydrophobic and hydrophilic by treating them with 0.1 and 0.01% DDS (dichlorodinethylsilane) solution in xylene for 1 h, respectively. Finally, the silanized surfaces were rinsed in sequence with 100 mL xylene,

acetone, and then ethanol. The plates were dried by blowing N_2 and were then stored in a desiccator. The chemically modified silicon surfaces are stable and perfectly suited for ellipsometry. The surface hydrophobicity is readily quantified using contact angle (wettability) methods (32).

3.4 Adsorption Kinetics

The adsorption kinetics data of proteins were monitored *in situ*, with ellipsometry (Model L116C, Gaertner Scientific Corp., Chicago, IL). The instrument was described in detail by Arnebrant (33), and the ellipsometric theory is described by McCrackin et al. (34). The ellipsometrically determined angles Ψ and Δ enable the calculation of thickness and refractive index of adsorbing layer by measuring changes in the state of polarized laser light reflected from a sample surface. Reflected light is characterized by Δ, defined as the change in phase, and the angle Ψ, which is the arctangent of the factor by which the amplitude ratio changes. Adsorbed mass was calculated from ellipsometrically-determined values of thickness and refractive index according to Cuypers et al. (35). As explained by Wahlgren and Arnebrant (36), the method requires protein-specific values of partial specific volume (v) and a ratio of molecular weight to molar refractivity (M/A) for each protein. These values for all Ile3 variants with identical 3-D structure were calculated as described by Pethig (37). The calculated values of M/A for Ile 3→Cys(S-S), wild type and Ile 3→Trp are 3.829, 3.827 and 3.825 g/cm^3, and that of partial specific volume 0.778, 0.78 and 0.778 cm^{-3}, respectively.

Silanized, bare surfaces were placed into a fused quartz trapezoid cuvette (Hellma Cells, Forest Hills, NY) having capacity of about 7 mL. Its fused quartz windows were placed normal to the path of the incident and reflected laser beams (angle of incidence = 70°, 1 mW helium-neon laser, wavelength 6328 Å). The ellipsometer sample stage was adjusted to get maximum reflection and then 5 mL of filtered buffer (0.01 M sodium phosphate buffer, pH 7.0) solution was injected into the cuvette. Fine adjustments of the stage were conducted to record steady values of Ψ and Δ for bare surface. After that buffer solution was carefully removed from the cuvette and replaced with 5mL of 1 mg/mL protein solution in the buffer. Ellipsometrically determined angles Ψ and Δ were recorded under static condition at intervals of about 30 s until the plateau was apparent (typically after 8 h). Recorded values of Ψ and Δ were used in computer program to determine film refractive index, thickness, and the adsorbed mass of protein on each surface (35).

At least three tests were performed with each type of surface to decrease experimental error associated with the results, and as average deviation of 0.03 $\mu g/cm^2$ from the mean was observed.

4. RESULTS AND DISCUSSION

4.1 Visual Analysis of Kinetic Plots

Representative plots of the adsorption kinetics exhibited by each of the proteins at hydrophobic and hydrophilic surfaces are shown in Figure 3 (a-c). Ile 3→Cys(S-S) and Ile 3→Trp adsorbed on both surfaces at about the same initial rate. In the case of wild type, the initial rate of adsorption is higher on the hydrophobic surface than that on the hydrophilic surface. The final adsorbed mass for all three proteins was higher on hydrophobic surfaces than on hydrophilic surfaces.

In all cases, adsorption can be considered as having proceeded in the absence of mass transfer limitations. Xu and Damodaran (12) measured an apparent diffusion coefficient for T4 lysozyme (0.15×10^{-11} m^2/s) which is about two orders of magnitude lower than that measured in solution. McGuire et al. (14) used penetration theory to indicate that diffusion-limited adsorption would yield a surface coverage of about 0.195 $\mu g/cm^2$ after 2 s. Analysis of Figure 3(a-c) shows that this rate is much greater than that visible for any of the plots.

The data in Figure 3 is replotted in Figure 4, to better illustrate the protein-specific differences in adsorption kinetics exhibited at hydrophobic and hydrophilic surfaces. In the case of the hydrophobic surface, wild type adsorbed faster, attaining the highest plateau, followed by Ile3→Cys(S-S) and then Ile3→Trp. The adsorbed mass after 8 h on both hydrophobic and hydrophilic surfaces decreased in the order wild type > Ile 3→Cys(S-S)

> Ile 3→Trp. Protein-specific differences in the initial adsorption rates were less obvious on the hydrophilic surface than on the hydrophobic surface.

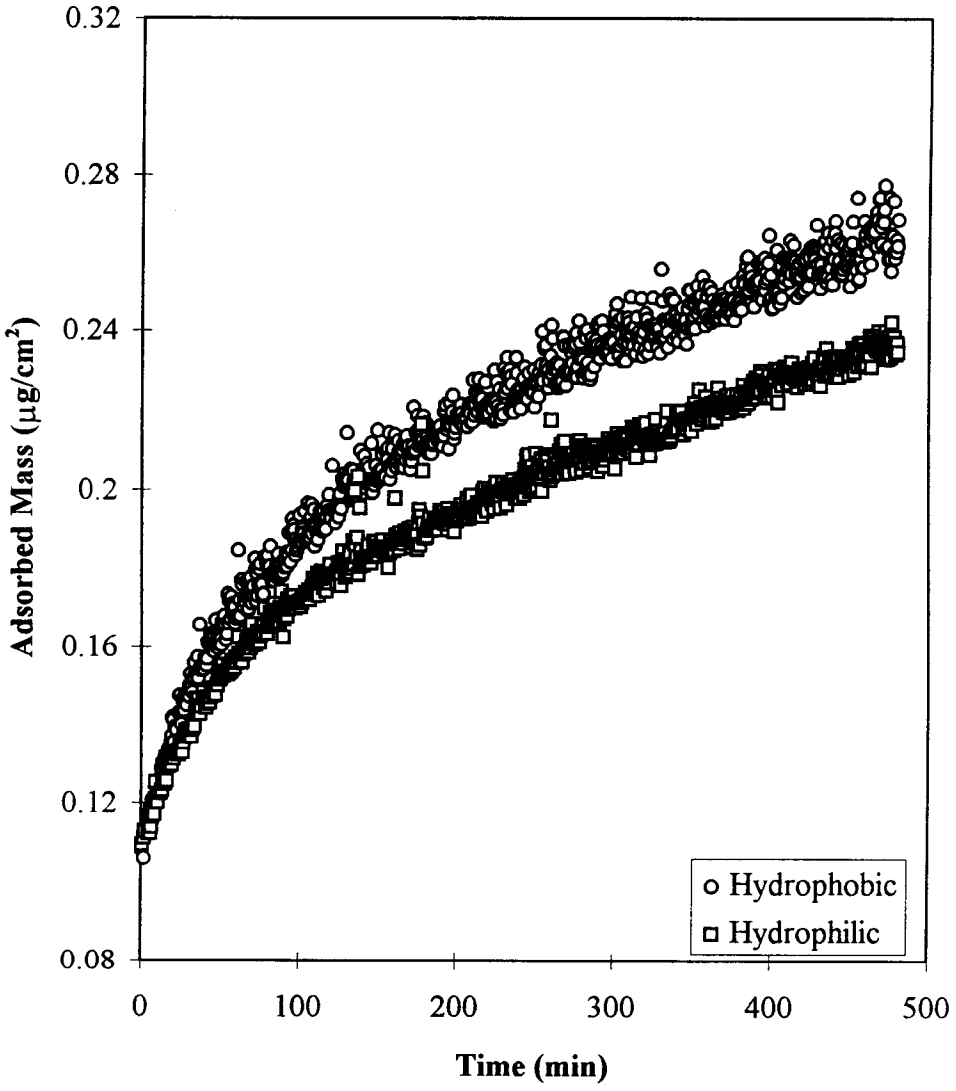

Figure 3(a). Adsorption kinetics of Ile3→Cys(S-S) on hydrophobic and hydrophilic surfaces.

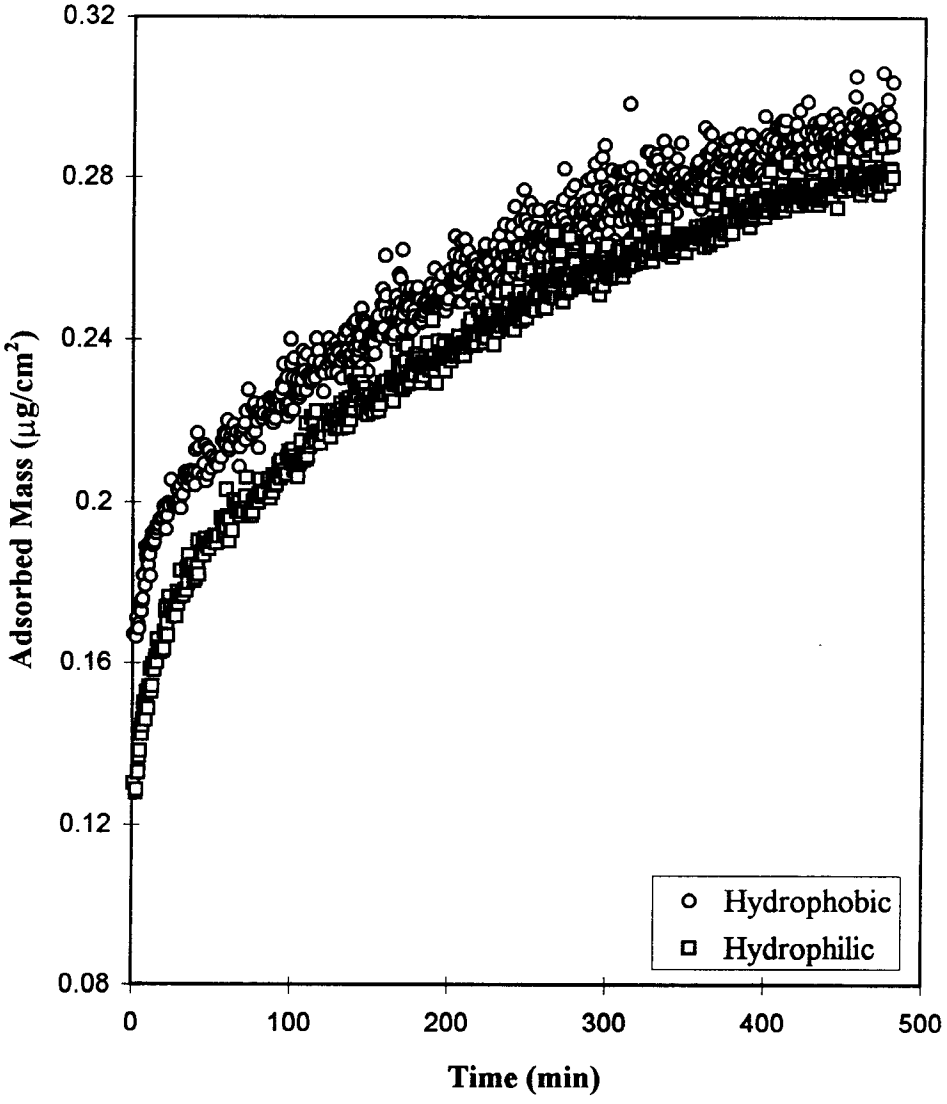

Figure 3(b). Adsorption kinetics of wild type on hydrophobic and hydrophilic surfaces.

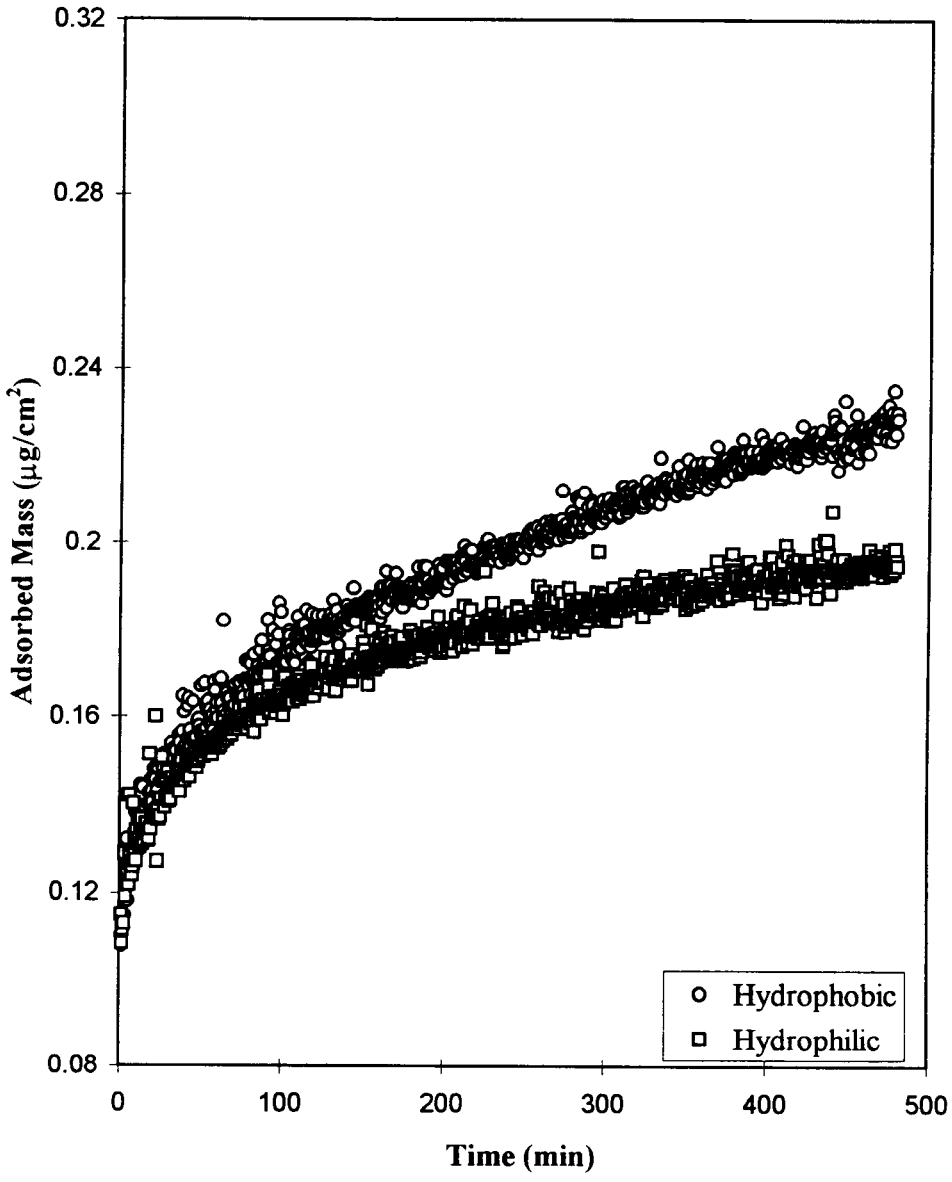

Figure 3(c). Adsorption kinetics of Ile3→Trp on hydrophobic and hydrophilic surfaces.

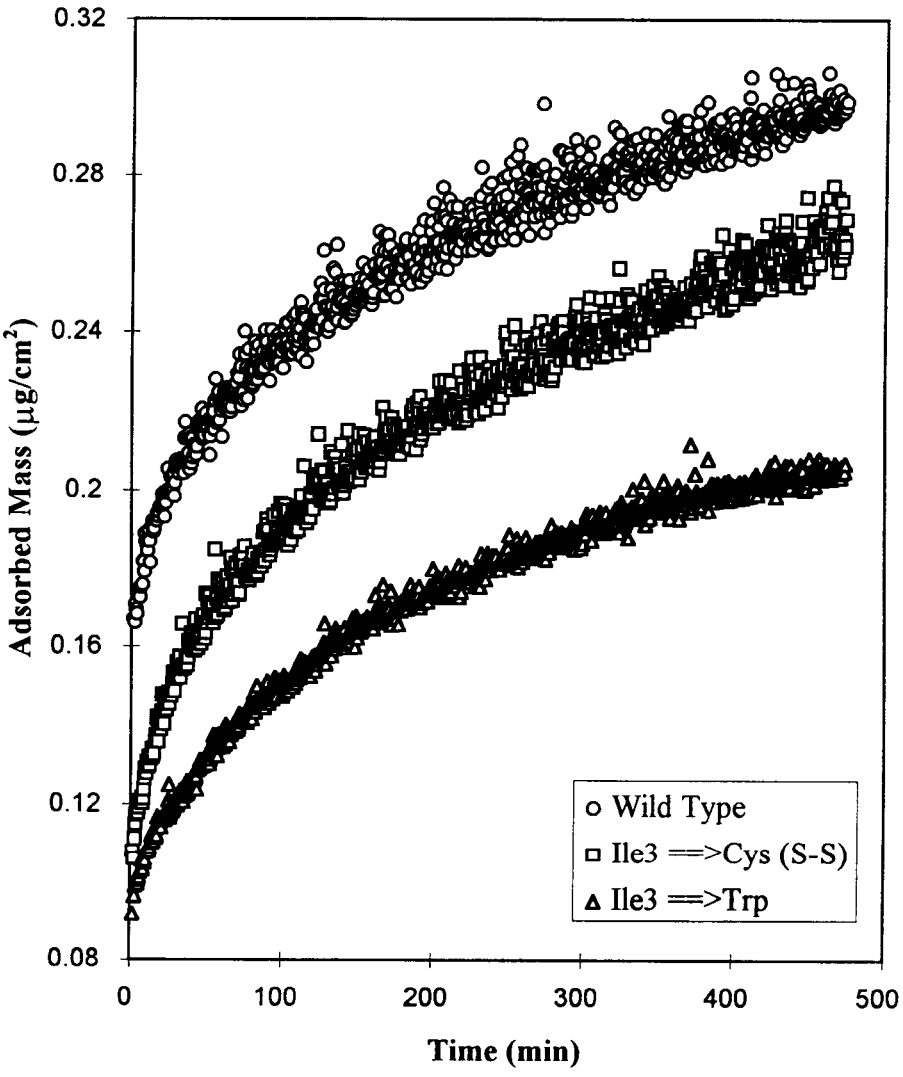

Figure 4(a). Comparison of adsorption kinetics of three proteins on a hydrophobic surface.

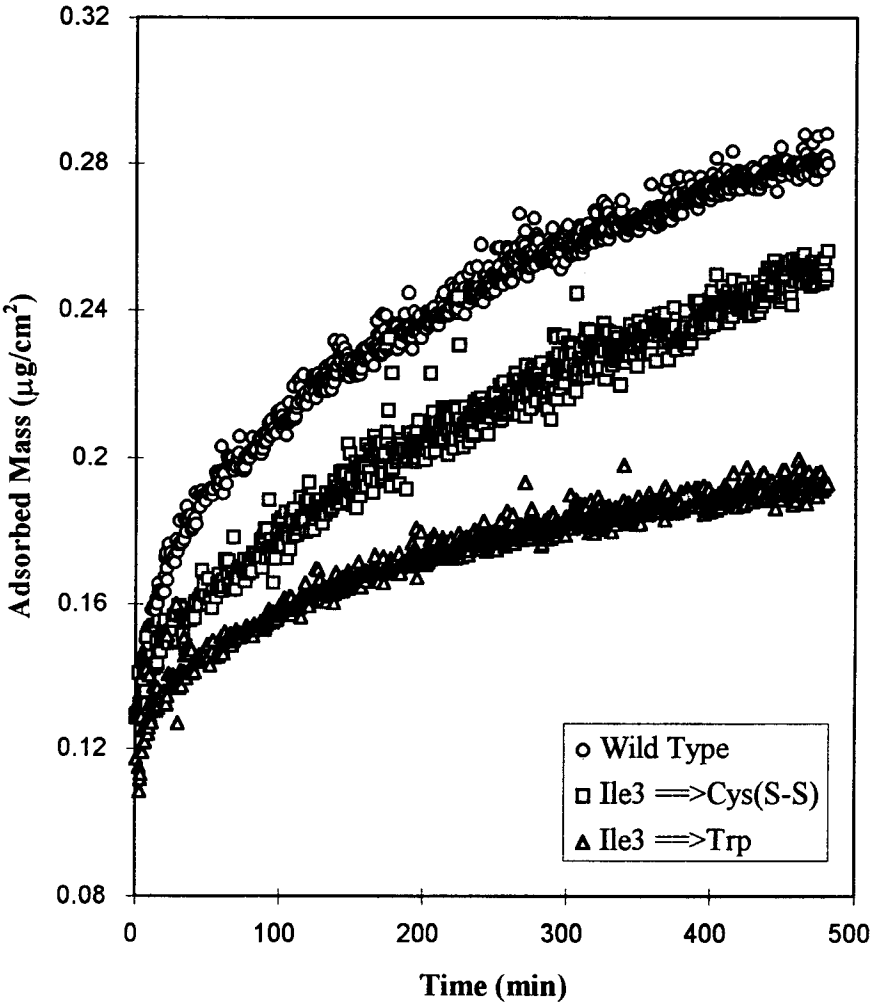

Figure 4(b). Comparison of adsorption kinetics of three proteins on a hydrophilic surface.

4.2 Comparison to Kinetic Models

4.2.1 Three-Rate-Constant Model: Models based on Langmuir-type behavior have been applied to explain features of protein adsorption at solid-liquid interfaces (38), but even modified forms of such models do not adequately account for the experimental results observed in a number of circumstances. A realistic model for protein adsorption behavior must take account of the dynamic behavior of protein molecules themselves. Lundström (39) proposed a mathematical model for reversible protein adsorption, based on a mechanism where protein molecules adsorb reversibly to the surface and undergo time-dependent unfolding. The model for protein adsorption adapted from this mechanism is complicated and only numerical solutions is possible, allowing simulation studies to be performed involving pertinent rate constants. Krisdhasima et al. (40) used a similar mechanism, but for irreversible adsorption, to explain adsorption kinetic behavior. In that mechanism, protein molecules initially adsorb reversibly on the surface, with a conformation close to their native form. After a sufficient time, a surface-induced conformational change transforms the reversibly adsorbed molecules to an irreversibly adsorbed form. An analytic solution of this model will provide us with the absolute measurements of the rate constants governing protein adsorption kinetics. This mechanism is shown in Figure 5. The following assumptions will be made regarding the mechanism of Figure 5.

1. The rate constants governing the initial, reversible adsorption, k_1 and k_{-1}, are assumed to be the same for all the synthetic stability mutants, and only surface rate constant, s_1, is mutant-dependent.

2. The conversion does not involve any change in interfacial area occupied by the molecule.

3. The surface is homogeneous, and no lateral interactions occur among neighboring molecules.

4. At maximum adsorption (the plateau in a kinetic plot), the surface is covered with a monolayer of protein molecules.

5. The resistance due to diffusion of protein molecules through the boundary layer is negligible.

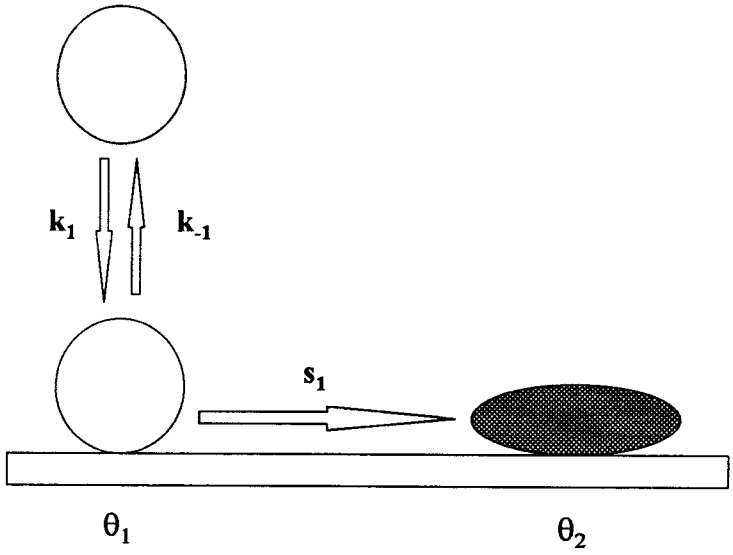

Figure 5. A simple, two-step mechanism for protein adsorption (40)

An expression for adsorbed mass as a function of time (t), protein concentration (C), and reaction rate constants k_1, k_{-1}, and s_1 as depicted in Figure 5, can be derived by first writing equations describing the rates of change of θ_1 and θ_2, where θ_1 and θ_2 are the fractional surface coverages of the molecules in state 1 and state 2 (40) :

$$\frac{d\theta_1}{dt} = k_1C\,(1-\theta_1-\theta_2) - (k_{-1}+s_1)\,\theta_1 \qquad \text{and} \qquad [1]$$

$$\frac{d\theta_2}{dt} = s_1\theta_1. \qquad [2]$$

Also, at any time, the total surface coverage is described by

$$\theta = \theta_1 + \theta_2. \qquad [3]$$

The surface coverages obey the initial condition that at $t = 0$, $\theta = \theta_1 = \theta_2 = 0$, as well as the final condition that at $t = \infty$, $\theta_1 = 0$ and $\frac{d\theta_2}{dt} = 0$.

The final analytical solution is of the form:

$$\theta_1 = c_1 \exp(-r_1t) + c_2 \exp(-r_2t) \qquad \text{and} \qquad [4]$$

$$\theta_2 = c_3 \exp(-r_1t) + c_4 \exp(-r_2t) + c_5 \qquad [5]$$

where the roots r_1 and r_2 for each equation above are given as

$$r_1 = (1/2)\,(k_1C + k_{-1} + s_1) + (1/2)\,([k_1C + k_{-1} + s_1]^2 - 4s_1k_1C)^{1/2} \qquad [6]$$

and

$$r_2 = (1/2)\,(k_1C + k_{-1} + s_1) - (1/2)\,([k_1C + k_{-1} + k_1]^2 - 4s_1k_1C)^{1/2} \qquad [7]$$

and the c_i are constants. The total surface coverage as a function of time is

$$\theta = \theta_1 + \theta_2 = A_1 \exp(-r_1t) + A_2 \exp(-r_2t) + A_3\,, \qquad [8]$$

where A_1, A_2 and A_3 are constants. An expression for the total adsorbed mass as a function of time can be obtained as

$$\Gamma = a_1 \exp(-r_1t) + a_2 \exp(-r_2t) + a_3. \qquad [9]$$

The parameters a_1, a_2 and a_3 are the products of Γ_{max}, the "equilibrium" adsorbed mass, with A_1, A_2 and A_3, respectively. Nonlinear regression performed on the adsorption kinetic

data fit to Eq. [9] would yield estimates of the parameters a_1, a_2, a_3, r_1 and r_2. Parameters r_1 and r_2 are related to the rate constants k_1, k_{-1} and s_1 according to

$$(r_1 + r_2) = (k_1C + k_{-1} + s_1) \quad \text{and} \quad [10]$$

$$r_1 r_2 = s_1 k_1 C \quad [11]$$

Table 1 lists average values of r_1 and r_2 and their product for each protein-surface contact. Due to its smaller magnitude, r_1 affects the kinetic curve for a longer time than r_2. The effect of parameter r_2, which is about two orders of magnitude greater than r_1, vanishes as time increases because the term $\exp(-r_2 t)$ rapidly approaches zero. Due to the disparity in the magnitudes of r_1 and r_2, Eq. [11] would provide the most useful information on adsorption kinetics. If it is hypothesized that the rate constants k_1 and k_{-1} are the same for all three proteins, with only s_1 being mutant dependent, then the product of r_1 and r_2 can be taken as an index of the surface rate constant, s_1. It is clear from Table 1 that the magnitude of $r_1 r_2$ increases with a decrease in protein stability and this effect is more pronounced on hydrophilic than on hydrophobic surfaces. These results are consistent with McGuire et al. (14). However, little difference is seen in comparison between wild type and Ile3→Cys(S-S).

Table 1. Average values of r_1 and r_2 for each protein on hydrophobic (HPB) and hydrophilic (HPL) surfaces.

Protein	$r_1 \times 10^3$		r_2		$r_1 r_2 \times 10^3$	
	HPB	HPL	HPB	HPL	HPB	HPL
Ile3→Cys(S-S)	6.63	3.23	0.81	0.98	5.37	3.17
Wild type	4.38	4.80	1.07	0.78	4.69	3.74
Ile3→Trp	6.42	5.68	1.21	1.57	7.77	8.92

4.2.2 Determination of Rate Constants and their Comparison to ΔΔG: By making use of the data from every possible pair of tests performed on a given surface, we can use equations [10] and [11] for each kinetic curve to yield four equations with four unknown variables. k_1 and k_{-1} are assumed not to change among these mutants, with only s_1 being affected by stability. A t-test was performed on calculated values of s_1 to determine 95% confidence interval, and hence this interval was used to eliminate data points that do not fall within the limit. Table 2 lists average values of s_1 along with their comparison with the ΔΔG values (27), for each protein-surface contact.

Table 2. Average values of s_1 compared to ΔΔG for each protein-surface contact.

Protein	ΔΔG [Kcal/mol]	s_1 [min^{-1}]	
		Hydrophobic	Hydrophilic
Ile 3→Cys(S-S)	+1.2	0.40	0.30
Wild type	0.0	0.43	0.47
Ile 3 → Trp	-2.8	0.70	1.03

On hydrophilic surfaces the magnitude of s_1 for Ile3→Cys(S-S) is about 35% lower, and for Ile3→Trp, about 120% higher than that for wild type. This implies that a protein of lower structural stability should more readily undergo a surface-induced structural change, all other things being equal. The higher magnitude of ΔΔG for Ile3→Trp as opposed to Ile3→Cys(S-S) is also consistent with its greater deviation in s_1 from the wild type. The deviation in s_1 values for all the Ile 3 variants is more pronounced on hydrophilic than on hydrophobic surfaces.

4.2.3 Comparison of the results to surfactant-mediated elution of these proteins:

Lundström and Elwing (41) developed a kinetic model in which bulk-surface exchange reactions involving two different proteins were considered. Adsorption to a solid surface was hypothetically allowed to occur from a single-component protein solution and after incubating it for some period, a second, dissimilar protein was added. In that model, after exchange, the adsorbed mass of the protein that resisted exchange was dependent upon its ability to change form at the interface. Krisdhasima et al. (13) made use of this development by adapting it to the sodium dodecylsulfate-mediated removal of selected milk proteins from silanized hydrophobic silica surfaces. The kinetic model led to an experimentally verifiable expression relating the fraction of the non-exchangeable form of adsorbed protein (θ_2) to rate constant s_1 (as defined in Figure 5), and to a rate constant (k_s) describing exchange of elutable protein by surfactant introduced to the solution. They considered adsorption of the protein to follow the mechanism shown in Figure 5, where adsorbed protein was considered to exist in either a removable or nonremovable form, and showed that after a sufficiently long time,

$$\frac{\theta_2}{\theta_{1,t_i}} = 1 - [k_s / (s_1 + k_s)] \cdot \exp(-s_1 t_s), \qquad [12]$$

Where θ_{1,t_i} is the value of θ_1 at $t = t_i$ (the initiation of adsorbed protein contact with clean buffer), and t_s is the time of surfactant addition. McGuire et al. (14) used dodecyltrimethylammonium bromide as surfactant to remove the same proteins used for the present experiments from silanized and unsilanized silica surfaces to quantify the effects of structural stability on their elution. In that work, the left side of Eq. [12], providing a measure of adsorbed protein binding strength, was experimentally estimated as

the mass of protein left at the end of an experiment, divided by the mass of protein present at the time of surfactant addition.

Eq. [12] can be rewritten for any two proteins as

$$\frac{(1-\frac{\theta_2}{\theta_{1,\,ti}})_{w.\,t.}}{(1-\frac{\theta_2}{\theta_{1,\,ti}})_{mutant}} = \exp(s_{1,\,mutant} - s_{1,\,w.t.})\; ts\; [(s_{1,\,mutant} + k_s)/(s_{1,\,w.t.} + k_s)] \qquad [13]$$

If for these extremely similar proteins k_s can be taken as protein-independent, the left side of Eq. [13] can be considered a function of s_1 alone, increasing with $s_{1,\,mutant}$. Table 3 shows the ratios of the surface rate constants (s_1) for each mutant relative for that of wild type, as calculated from Table 2, compared to the values of the left side of Eq. [13], using data of McGuire et al. (14).

Table 3. The ratio $s_{1mutant}/s_{1w.t.}$ compared to surfactant-mediated elution data by McGuire et al. (14).

Protein	$\frac{(s_{1,\,mutant})}{(s_{1,\,w.t.})}$		$\frac{(1-\frac{\theta_2}{\theta_{1,\,ti}})_{w.\,t.}}{(1-\frac{\theta_2}{\theta_{1,\,ti}})_{mutant}}$	
	Hydrophobic	Hydrophilic	Hydrophobic	Hydrophilic
Ile 3→Cys(S-S)	0.93	0.64	0.94	0.90
Wild type	1.00	1.00	1.00	1.00
Ile 3→Trp	1.63	2.19	1.10	1.55

It is clear from Table 3 that on each surface, the ratio $\frac{(s_{1,\,mutant})}{(s_{1,\,w.t.})}$ increased with the ratio on the right side of Table 3. Both the ratios increased faster on hydrophilic surfaces than on hydrophobic surfaces. The overall increase for the ratio based on surfactant-

mediated elution data is slower as we would expect for $k_s >> s_1$. Both ratios increased with decreasing protein stability. Thus we would conclude that a less stable protein would more readily make the conversion from the removable to the nonremovable (i.e., more tightly bound) form, and this is more pronounced on hydrophilic than on hydrophobic surfaces.

4.2.4 Parallel Adsorption Model: The model [9] just discussed was applied assuming that molecules in their nonremovable form are generated only after being adsorbed in their removable form, and that the conversion did not involve any change in interfacial area occupied by the molecule. The pattern of data in the present experiments is such that the initial kinetics as well as the total mass adsorbed after 8 h differ among the proteins, indicating that adsorption of the more tightly bound state may occur rather quickly, and molecules in that state may occupy more interfacial area. Therefore, the mechanism shown in Figure 6, allowing protein to adopt one of two states directly from solution, was considered. The state 1 molecules are defined as less tightly bound, occupying less interfacial area than those in state 2. We will define A_1 as the interfacial area occupied by a state 1 molecule while A_2 is that for a state 2 molecule. This mechanism was used to assist interpretation of adsorption and elution data of T4 lysozyme charge and stability mutants (9,14), and showed that state 2 molecules were more resistant to elution than those in state 1. Moreover, for wild type, Ile3→Cys(S-S) and Ile3→Trp, elution from each state was protein-independent.

As shown in Figure 6, protein adsorption is proposed to occur by two parallel reactions. Adsorption in state 1 and state 2 are governed by rate constants k_1 and k_2, respectively.

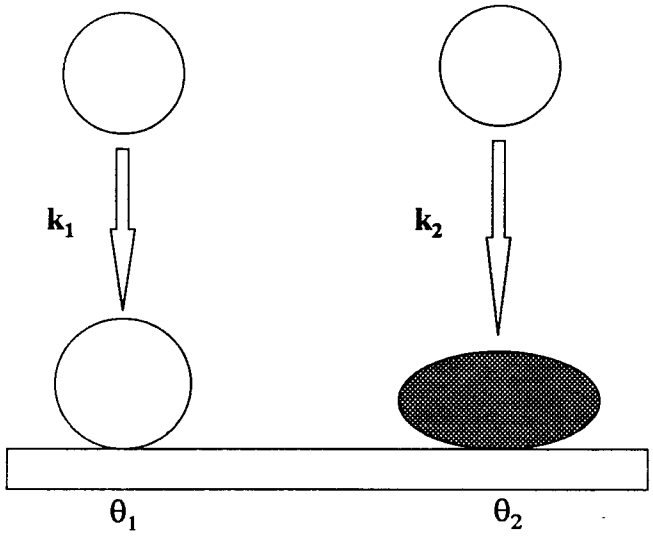

Figure 6. A simple mechanism for T4 lysozyme adsorption into one of two states defined by fractional surface coverages θ_1 and θ_2.

An expression for adsorbed mass as a function of protein concentration (C), reaction rate constants k_1 and k_2, and time is derived by first writing equations describing the time-dependent fractional surface coverage of protein in each of the two states as

$$\frac{d\theta_1}{dt} = k_1 C\,(1 - \theta_1 - a\theta_2) \qquad [14]$$

and

$$\frac{d\theta_2}{dt} = k_2 C\,(1 - \theta_1 - a\theta_2). \qquad [15]$$

θ_1 and θ_2 are redefined as the mass of molecules adsorbed ($\mu g/cm^2$) in state 1 and state 2, respectively, each divided by Γ_{max}, where Γ_{max} is the maximum mass of molecules that

could be adsorbed in a monolayer. Parameter a defined as A_2/A_1 is estimated as $\Gamma_{max}/\Gamma_{max,side\text{-}on}$, because the adsorption kinetic data are all close to side-on to somewhere between side-on and end-on. Parameter a was set equal to 2.11 (= 0.396/0.188) on hydrophilic surfaces, where 0.396 $\mu g/cm^2$ corresponds to a monolayer of molecules adsorbed end-on, and 0.188 $\mu g/cm^2$ is the average plateau attained by Ile3→Trp molecules at the hydrophilic surface. On hydrophobic surfaces, this value is 0.199 $\mu g/cm^2$, and a was set equal to 1.99 (= 0.396/0.199). The magnitude of $\Gamma_{max,side\text{-}on}$ used in estimation of a is less than that calculated based on dimensions of the molecules in solutions (= 0.205 $\mu g/cm^2$). This is because the lowest values of adsorbed mass obtained, i.e., for Ile3→Trp, were slightly lower than that expected for side-on. It is assumed here that the surface is covered with molecules that are slightly more spread than we would expect in solution. The solution of Equations [14] and [15] with two roots, $root_1 = 0$ and $root_2 = -(ak_2C+k_1C)$ is given as

$$\theta_1 + \theta_2 = d_1 + d_2 \exp[-(ak_2C + k_1C)] \qquad [16]$$

where d_1 and d_2 can be evaluated from the boundary conditions, and the definition of θ_1 and θ_2 requires that

$$\theta_1 + a\,\theta_2 = 1 \qquad [17]$$

$$\text{and also } \frac{k_2}{k_1} = \frac{\theta_2}{\theta_1}, \text{ as } t \rightarrow \infty \qquad [18]$$

The final form of the model becomes

$$\Gamma = \Gamma_{max} \frac{k_1C + k_2C}{k_1C + ak_2C} \{1-\exp[-(k_1C + ak_2C)t]\} \qquad [19]$$

Eq. [19] can be rewritten as

$$\Gamma = b\{1\text{-}\exp[-(c)t]\} \qquad [20]$$

Nonlinear regression performed on the adsorption kinetic data fit to Eq. [20] would yield estimates of the parameters b and c, which are related to k_1 and k_2 according to

$$b = \Gamma_{max} \frac{k_1C + k_2C}{k_1C + ak_2C} \quad \text{and} \qquad [21]$$

$$c = k_1C + ak_2C \qquad [22]$$

Table 4 lists average values of k_1C and k_2C and the comparison of k_2/k_1 to the s_1 values calculated earlier for each protein-surface contact. The ratio k_2/k_1 indicates the number of molecules that are in state 2 relative to the number of molecules that are in state 1. Higher values of k_2/k_1 are consistent with lower plateaus in the kinetic plots, because the molecules in state 2 occupy greater interfacial area than those in state 1.

Table 4. Averaged k_1C and k_2C from parallel adsorption model and the comparison of their ratio, k_2/k_1 with s_1 on each of hydrophobic (HPB) and hydrophilic (HPL) surfaces.

Protein	$k_1C \times 10^3$ (mg/mL-min)		$k_2C \times 10^3$ (mg/mL-min)		k_2/k_1		s_1	
	HPB	HPL	HPB	HPL	HPB	HPL	HPB	HPL
Ile 3→Cys(S-S)	5.33	6.13	6.30	9.17	1.18	1.50	0.40	0.30
Wild type	8.18	21.97	13.23	37.6	1.62	1.71	0.43	0.47
Ile 3→Trp	7.65	7.23	17.5	23.85	2.29	3.3	0.70	1.03

In Table 4 the expected trend is observed in the values of k_2/k_1 and s_1 on both the hydrophobic and hydrophilic surfaces, i.e., the tendency of a protein to adopt state 2 increases with decreasing structural stability. Figure 7 (a-c) illustrates the variation between the experimentally determined adsorbed mass vs. time for each protein and the

adsorbed mass vs. time calculated by using Eq. [19]. The model underestimates the final adsorbed mass in the cases of Ile3→Cys(S-S) and wild type, but overestimates it for Ile3→Trp.

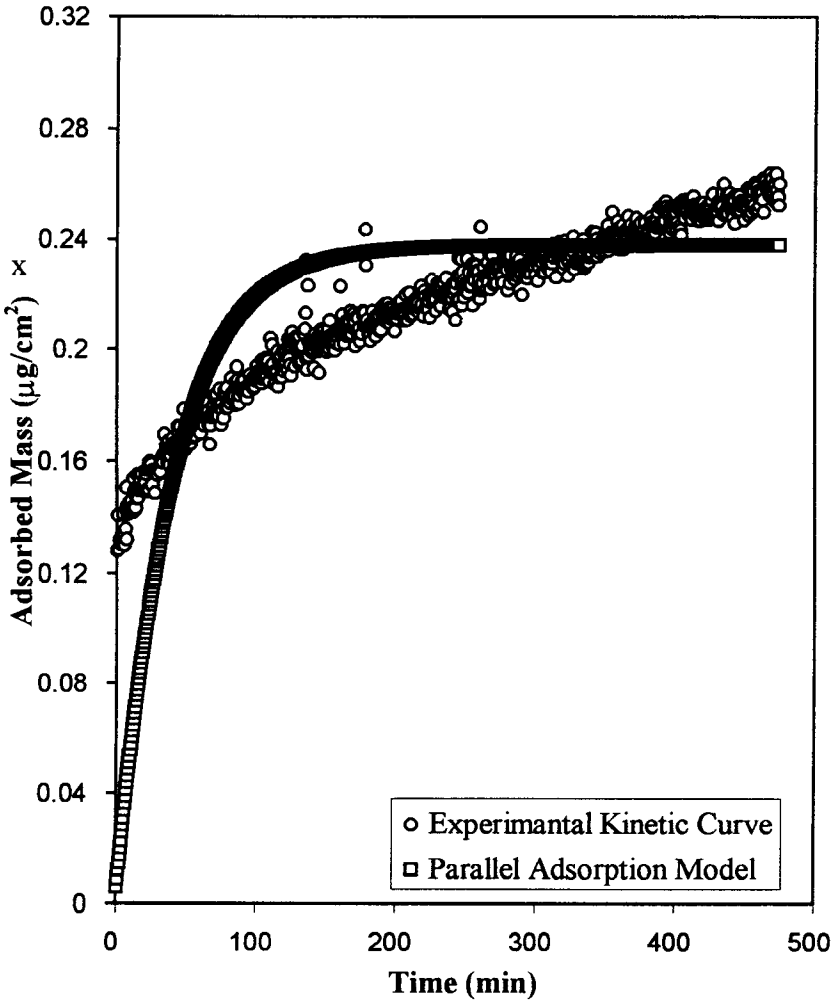

Figure 7(a). Comparison of adsorption kinetics observed experimentally with that predicted by parallel adsorption model, for Ile3→Cys(S-S).

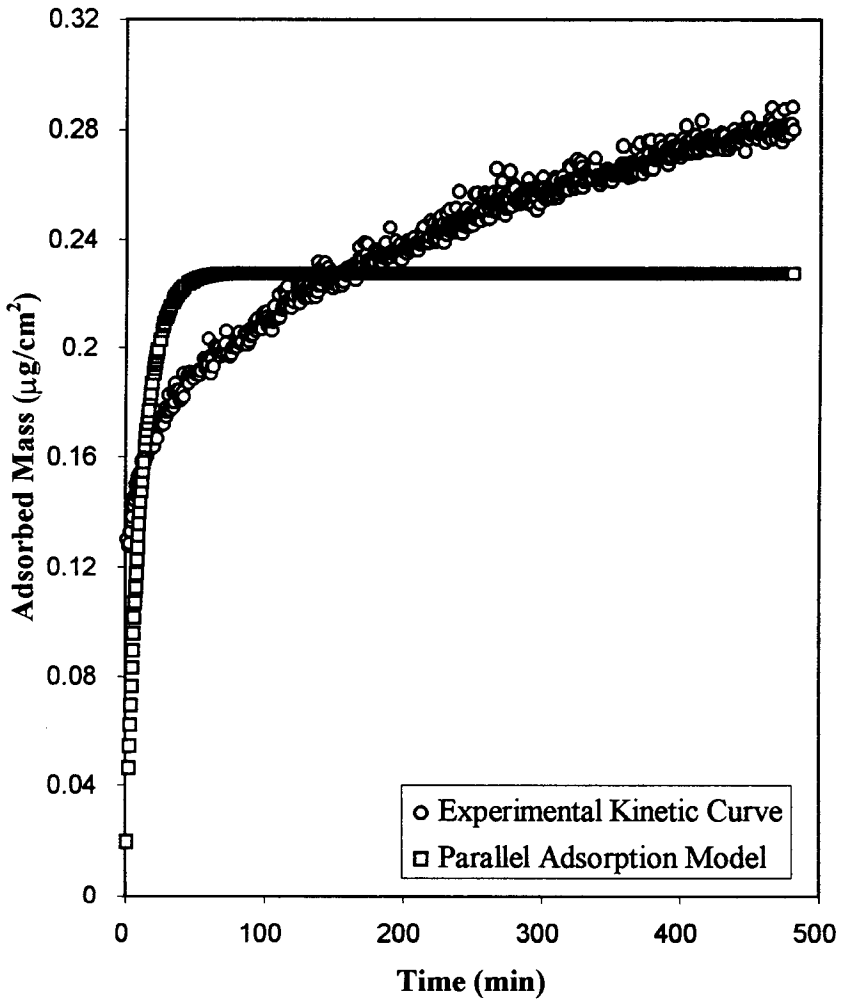

Figure 7(b). Comparison of adsorption kinetics observed experimentally with that predicted by parallel adsorption model, for wild type.

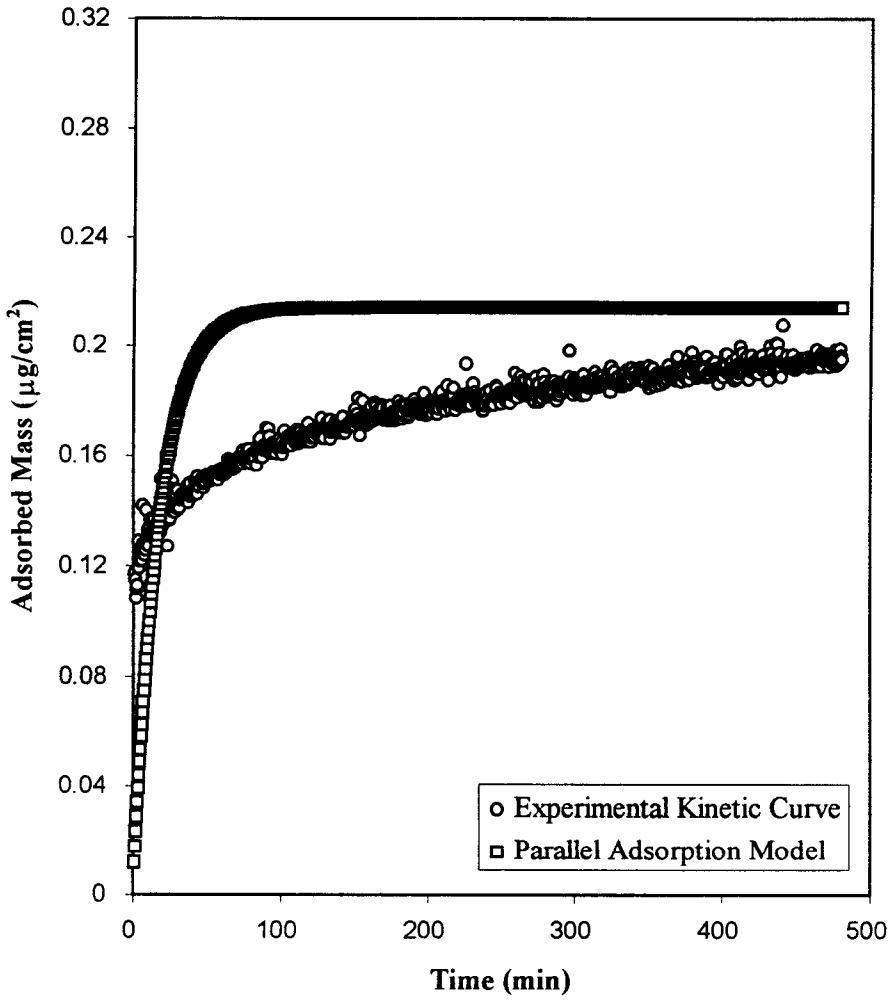

Figure 7(c). Comparison of adsorption kinetics observed experimentally with that predicted by parallel adsorption model, for Ile3→Trp. Figure 7(c).

The data were analyzed by linear regression to better fit the plateau regions, and Eq. [20] was rewritten as

$$\ln(b-\Gamma) = \ln(b) - (c)t \qquad [23]$$

A careful analysis of the plots of $(b-\Gamma)$ vs. t on semi-log coordinates indicated that the data recorded after t= 60 min were linear. Therefore, for each run, the intercept (fixed as the experimentally-determined adsorbed mass at t= 8 h, or $\Gamma_{max}\frac{k_1C + k_2C}{k_1C + ak_2C}$) along with the slope $(k_1C + k_2C)$ of the semi-log plot constructed for t= 61-480 were used to calculate k_1C and k_2C. Average values of k_1C and k_2C are shown in Table 5.

Table 5. Averaged k_1C and k_2C from linearized model and the comparison of their ratio, k_2/k_1 with s_1 on each of hydrophobic (HPB) and hydrophilic (HPL) surfaces.

Protein	$k_1C \times 10^4$		$k_2C \times 10^4$		k_2/k_1		s_1	
	HPB	HPL	HPB	HPL	HPB	HPL	HPB	HPL
Ile 3→Cys(S-S)	4.13	3.88	2.77	2.81	0.67	0.72	0.40	0.30
Wild type	3.03	2.02	2.18	1.87	0.72	0.95	0.43	0.47
Ile 3→Trp	1.04	0.62	2.88	2.60	2.77	4.19	0.70	1.03

Again, k_2/k_1 is higher on hydrophilic than on hydrophobic surface for each protein, and Ile 3→Trp on the hydrophilic surface has the maximum value of this ratio. This would imply that more molecules adopt the more tightly bound state, i.e., state 2, as stability is decreased, and is exactly in line with the observation from the three-rate-constant model, stating that less stable protein is more likely to be adsorbed in state 2. This effect is more pronounced on hydrophilic as opposed to hydrophobic surfaces.

A comment about the validity of the mechanisms:

This discussion is consistent with the thought that Ile3→Trp adsorbs and adopts state 2 quickly, even when the surface is crowded with molecules, whereas other proteins arrive on the surface and adopt state 2 at a slower rate. Billsten et al. (15) supported this by showing that Ile3→Trp makes extreme losses in secondary structure upon adsorption, and McGuire et al. (14) stated that Ile3→Trp is not only the most resistant to elution but also completely adsorbed in state 2 at the time of surfactant addition. If the concentration of protein is lowered by 100 fold they would likely all adopt state 2 because of the absence of neighboring molecules (31). In this case we would expect that method (sequential addition of protein to the final concentration of 1mg/mL vs. single-step addition of protein at concentration 1mg/mL) of recording final plateau is less important for Ile3→Trp.

Adsorption to a solid surface was allowed to occur, first from a protein solution of concentration 0.01 mg/mL for four hours, followed by incubation in buffer, after which time the same protein at a concentration 0.1 mg/mL was added. Finally, after four hours, in the third step, protein at a concentration 1mg/mL is added following the same procedure. The results obtained for all the three proteins and their comparison with single step protein adsorption from a solution of 1 mg/mL are shown in Figure 8 (a-c). It is evident from Figure 8 that in all the Ile3 variants sequential addition of protein to the final concentration of 1 mg/mL yields a lower plateau than single step addition. But for Ile3→Trp as shown in Figure 8c, the plateau values from both the experiments are similar to each other, which is consistent with application of these models in this work.

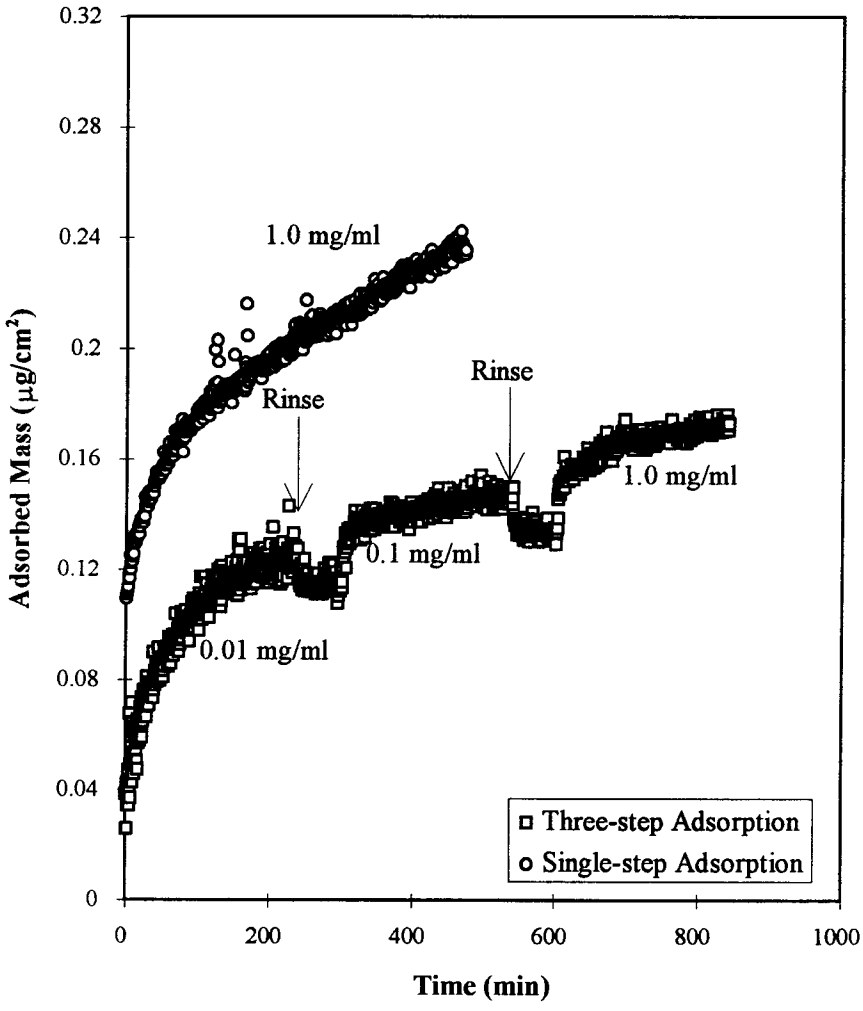

Figure 8(a). Comparison of single-step protein adsorption kinetics with the sequential addition of protein to the final concentration 1.0 mg/ml, for Ile3→Cys(S-S).

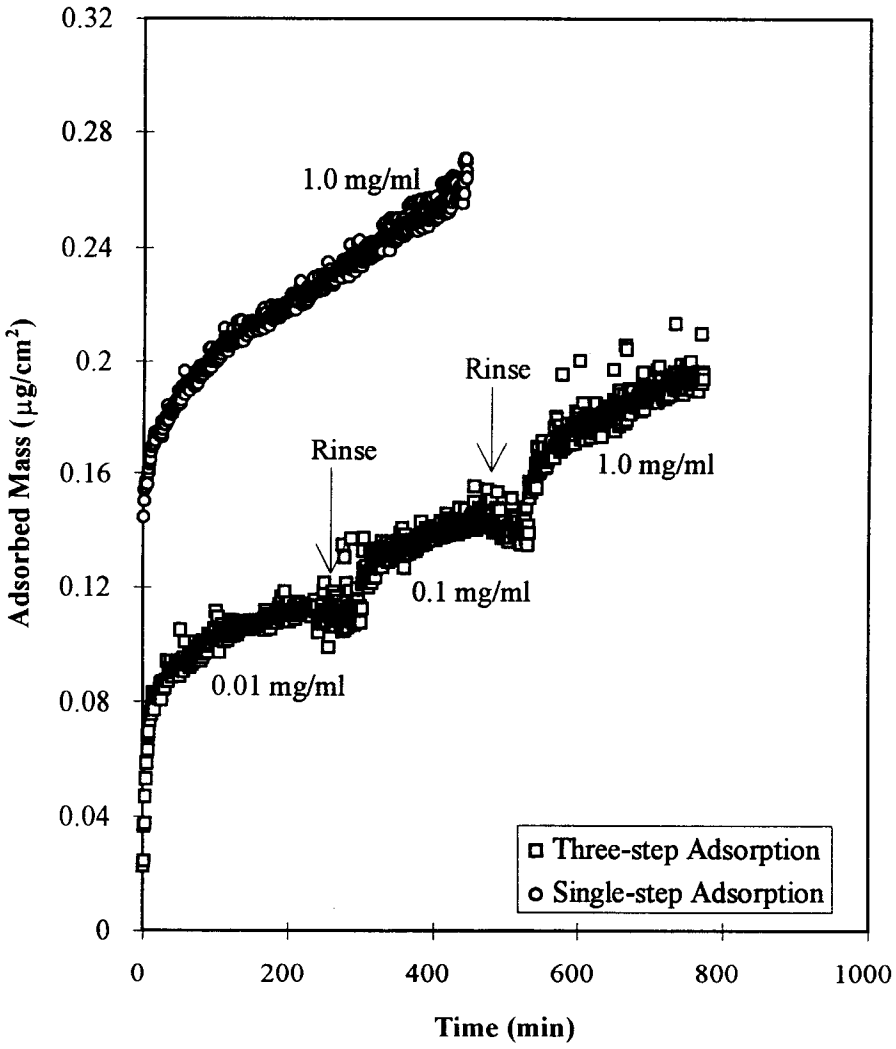

Figure 8(b). Comparison of single-step protein adsorption kinetics with the sequential addition of protein to the final concentration 1.0 mg/ml, for wild type.

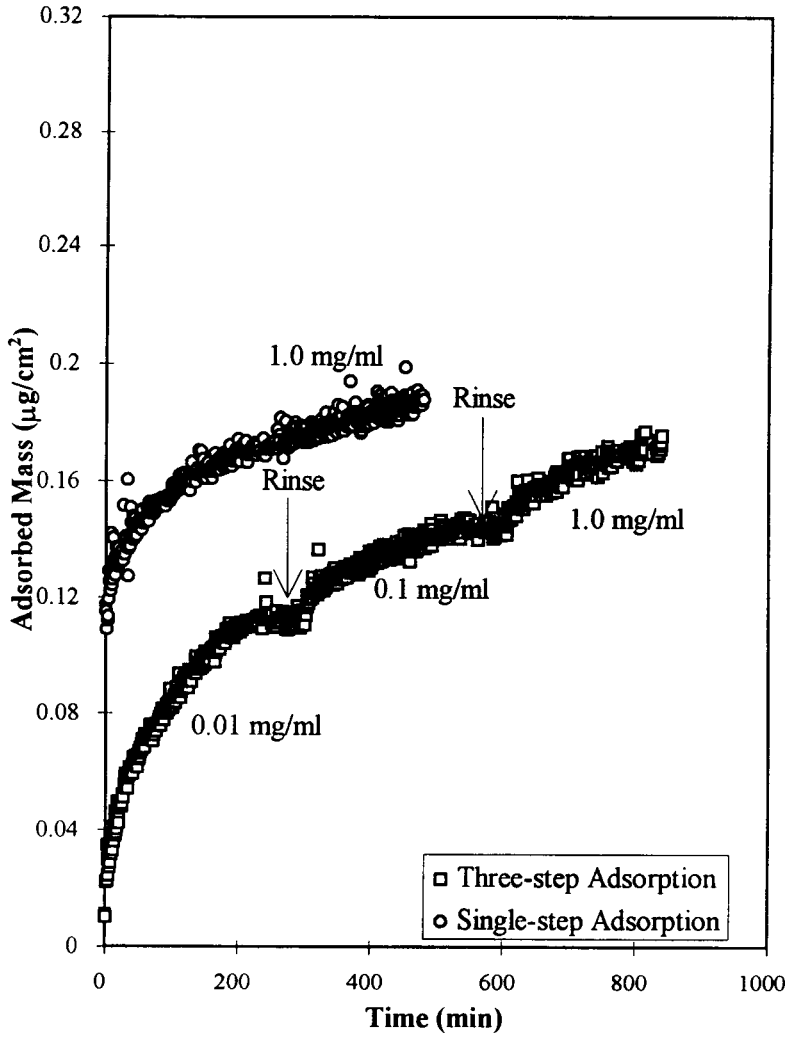

Figure 8(c). Comparison of single-step protein adsorption kinetics with the sequential addition of protein to the final concentration 1.0 mg/ml, for Ile3→Trp.

BIBLIOGRAPHY

1. Fane, A. G., Kim, K. J., Fell, C. J. D., and Suki, A. B., *in* "Characterization of Ultra Filtration Membranes" (G. Tradgardh, Ed.), p. 39. Proceedings from an international workshop arranged by Department of Food Engineering, Lund University, Sweden, 1987.

2. Andrade, J. D., *in* "Protein Adsorption" (J. D. Andrade, Ed.), p. 1-80. Plenum Press, New York, 1985.

3. Creighton, T. E., *Proteins, Structures and Molecular Properties*, W. H. Freeman, New York, 1984.

4. Shirahama, H., Lyklema, J., and Norde, W., *J. Colloid Interface Sci.* **139**, 177 (1990).

5. Wei, A. P., Herron, J. N., and Andrade, J. D., *in* "Biotherapie" (D. J. A. Crommelin, Ed.), in press.

6. Hunter, J. R., Carbonell, R. G., and Kilpatrick, P. K., *J. Colloid Interface Sci.* **143**, 37 (1991).

7. Horsley, D., Herron, J., Hlady, V., and Andrade, J. D., *in* "Proteins at Interfaces: Physicochemical and Biochemical Studies" (J. L. Brash and T. A. Horbett, Eds.), p. 290. ACS Symposium Series 343, Washington, D.C., 1987.

8. Kato, A., and Yutani, K., *Protein Engineering* **2**, 153 (1988).

9. McGuire, J., Wahlgren, M. C., and Arnebrant, T. (1995) The influence of net charge and charge location on the adsorption and dodecyltrimethylammonium bromide-mediated elutability of bacteriophage T4 lysozyme at silica surfaces, *J. Colloid Interface Sci.*, in press.

10. Asakura, T., Ohnishi, T., Friedman, S., and Schwartz, E., *Proc. Nat. Acad Sci.* USA. **71**, 1594 (1974).

11. Adachi, K. and Asakura, T., *Biochemistry*. **13**, 4976 (1974).

12. Xu, S. and Damodaran, S., *J. Colloid Interface Sci.* **159**, 124 (1993).

13. Krisdhasima, V., Vinaraphong, P. and McGuire, J., *J. Colloid Interface Sci.* **161**, 325 (1993).

14. McGuire, J., Wahlgren, M. C., and Arnebrant, T. (1995) Structural stability effects on the adsorption and dodecyltrimethylammonium bromide-mediated elutability of bacteriophage T4 lysozyme at silica surfaces, *J. Colloid Interface Sci.*, in press.

15. Billsten, P., Wahlgren, M., Arnebrant, T., McGuire, J., and Elwing, H., *J. Colloid Interface Sci.*, in review.

16. Matthews, B. W., Dahlquist, F. W., and Maynard, A. Y., *J. Mol. Biol.* **78**, 575 (1973).

17. Tsugita, A., *Phage lysozymes and other lytic enzymes*. In "The Enzymes", **5**, 343 411 (1971).

18. Koch, G., and Dreyer, W. J., *Characterization of an enzyme of phage T2 as a lysozyme*. Virology, **6**, 291-293 (1958).

19. Koch, G., and Jordan, E. M., *Killing of E. coli B by phage-free T2 lysates.* Biochim. Biophys. Acta, **25**, 437 (1957).

20. Weaver, L. H., and Matthews, B. W., Structures of bacteriophage T4 lysozyme refined at 1.7 Å resolution. *J. Mol. Biol.* **193**, 189-199 (1987).

21. Alber, T., and Matthews, B. W., *Meth. Enzymol.* **154**, 511 (1987).

22. Daopin, S., Liao, D-I., and Remington, S. J., Electrostatic fields in the active sites of lysozymes. *Proc. Natl. Acad. Sci.* U.S.A. **86**, 5361 (1989).

23. Dao-pin, S., Söderlind, E., Baase W. A., Wozniak, J. A., Sauer, U. and Matthews, B. W., submitted to *J. Mol. Biol.*

24. Alber, T., Daopin, S., Nye, J. A., Muchmore, D. C., and Matthews, B. W., Temperature sensitive mutations of bacteriophage T4 lysozyme occur at sites with low mobility and low solvent accessibility in the folded protein. *Biochemistry.* **26**, 3754-3758 (1987).

25. Grutter, M. G., and Matthews, B. W., *J. Mol. Biol.* **154**, 525 (1982).

26. Matsumura, M., and Matthews, B. W., *Science.* **243**, 792 (1989).

27. Matsumura, M., Becktel, W. J., and Matthews, B. W., *Nature* **334**, 406 (1988).

28. Muchmore, D. C., McIntosh, L. P., Russell, C. B., Anderson, D. E., and Dahlquist, F. W., *Meth. Enzymol.* **177**, 44 (1989).

29. Poteete, A. R., Dao-pin, S., Nicholson, H., and Matthews, B. W., *Biochemistry.* (1990).

30. Jönsson, U., Ivarsson, B., Lundström, I., and Berghem, L., *J. Colloid Interface Sci.* **90**, 148 (1982).

31. Wahlgren, M. C. and Arnebrant, T., J. *Colloid Interface Sci.* **136**, 259 (1989).

32. McGuire, J., Lee, E. and Sproull, R. D., *Surf. Interface Anal.* **15**, 603 (1990).

33. Arnebrant, T., Ph.D. Thesis, Lund University, Sweden (1987).

34. McCrackin, F., Passaglia, E., Stromberg, R. and Steinberg, H., *J. Res. NBS - A. Physics and Chemistry* **67A**, 363 (1963).

35. Cuypers, P., Corsel, J., Janssen, M., Kop, J., Hermens, W., and Hemker, H., *J. Biol. Chem.* **258**, 2426 (1983).

36. Wahlgren, M. C. and Arnebrant, T., *J. Colloid Interface Sci.* **142**, 503 (1991).

37. Pethig, R., *in* "Dielectric and Electronic Properties of Biological Materials" (R. Pethig, Ed.), p. 64. John Wiley & Sons, New York, 1979.

38. Adamson, A. W., *Physical chemistry of surfaces*, 4th Edition, Wiley, New York 1983.

39. Lundström, I., *Progr. Colloid Polymer Sci.* **70**, 76 (1985).

40. Krisdhasima, V., McGuire, J., and Sproull, R., *J. Colloid Interface Sci.* **154**, 337 (1992).

41. Lundström, I., and Elwing, H., *J. Colloid Interface Sci.* **136**, 68 (1990).

APPENDICES

APPENDIX A

Preparation of Broths

Recipes for preparation of 100 mL overnight broth (LB-H broth) and 4.8 liters fermentation broth (LB broth) are given in Table 6.

Table 6. Preparation of LB-H broth (overnight broth) and LB broth (fermentation broth).

Materials	LB-H broth	LB broth
Tryptone (g)	57.6	2.0
NaCl (g)	48.0	1.0
Yeast extract (g)	24.0	1.0
Glucose (g)	4.8	0.0
Distilled water (L)	4.8	0.2
1N NaOH (mL)	0.0	0.2

APPENDIX B

Preparation of Buffers and Solutions

Recipes of buffers and solutions used in this research are given in Table 7.

Table 7. Preparation of buffers and solutions.

Buffers/Solutions	pH	Preparation
0.1M Phosphate Buffer	6.5	0.711 g mono + 1.3785 g di-phosphate + 0.03 g NaN_3 + 4.82 g NaCl + 150 mL DDW
10 mM Phosphate Buffer	7.0	2.21 g mono in 1600 mL DDW titrated against 3.55 g di-phosphate in 2500 mL DDW to pH 7.0, add 0.8 g NaN_3
50 mM Phosphate Buffer	5.8	25.087 g mono + 2.58 g di-phosphate + 4L DDW + 0.8 g NaN_3
Lysis Buffer	6.6	2.07 g mono + 1.42 g di-phosphate + 2.92 g NaCl + 0.508 g $MgCl_2$ + 250mL DDW
10 mM Tris Buffer	7.4	0.132 g Tris acid + 0.091 g Tris base + 100 mL DDW
50 mM Tris Buffer	7.25	6.49 g Tris acid + 0.74 g Tris base + 1L DDW
50 mM NaCl in Tris		1.227 g NaCl + 420 mL 50 mM Tris
0.3M NaCl in Tris		7.889 g NaCl + 450 mL 50 mM Tris
10 mM HCl		0.1 mL HCl + 120 mL DDW
1.0 M $MgCl_2$		20.33 g $MgCl_2$ + 100 mL DDW
0.5 M EDTA	8.0	14.61 g EDTA + 100 mL DDW, use NaOH pellet to adjust pH to 7.2 at 80°C, then cool down and add DDW or 1N NaOH to 100 mL to adjust pH to 8.0

APPENDIX C

Values of Parameters r_1 and r_2 from Three-Rate-Constant Model

The parameters r_1 and r_2 are directly estimated by non-linear regression analysis of the experimental data fit to the Three-Rate-Constant Model and are given for each protein-surface contact in Table 8.

Table 8. Values of parameters r_1 and r_2 from Three-Rate-Constant Model.

Run Name	$-r_1 x 10^3$	$-r_2$
cys\1	4.9	1.192
cys\2	5.6	0.617
cys\3	8.7	0.564
cys\4	7.3	0.847
cysl\1	3.1	0.759
cysl\2	3.1	0.962
cysl\3	3.5	1.209
wild\1	5.1	1.019
wild\2	3.1	1.021
wild\3	4.4	1.110
wild\4	4.9	1.119
wildl\1	4.6	0.697
wildl\2	5.1	0.750
wildl\3	4.7	0.890
trp\1	4.2	1.150
trp\2	5.6	0.948
trp\3	9.0	1.059
trp\4	8.1	1.447
trp\5	5.2	1.440
trpl\1	6.0	1.377
trpl\2	5.9	1.940
trpl\3	6.8	1.516
trpl\4	4.0	1.440

APPENDIX D

Averaged Values of s_1 on Hydrophobic Surfaces from Three-Rate-Constant Model

Values of s_1 calculated from all successful runs are presented in Table 9.

Table 9. Average values of s_1 for each protein on hydrophobic surfaces.

	Ile3→Cys(S-S)	Wild Type	Ile3→Trp
s_1	0.505	0.620	0.951
	0.378	0.243	0.584
	0.526	0.308	0.729
	0.253	0.247	0.377
	0.348	0.159	0.066
	0.395	0.955	0.590
	0.671	0.343	0.098
	0.249	0.879	0.775
	0.256	0.291	1.200
		0.422	0.622
		0.205	1.128
			0.206
			0.514
			1.021
			0.699
			1.181
			0.608
			1.272
n	9	11	18
Average s_1	0.40	0.43	0.70

The magnitude of k_1C and k_{-1} on hydrophobic surfaces was calculated to be 0.013 min^{-1} and 0.63 min^{-1}, respectively while the corresponding values on hydrophilic surfaces were 0.009 min^{-1} and 0.44 min^{-1}. In each case, the ratio k_{-1}/k_1C, related to the reversible rate constant, was quite similar.

APPENDIX E

Averaged Values of s_1 on Hydrophilic Surfaces from Three-Rate-Constant Model

Values of s_1 for each protein calculated from all successful runs are presented in Table 10.

Table 10. Average values of s_1 for each protein on hydrophilic surfaces.

	Ile3→Cys(S-S)	Wild Type	Ile3→Trp
s_1	0.170	0.542	1.169
	0.247	0.598	1.220
	0.306	0.453	1.114
	0.225	0.432	1.192
	0.471	0.484	0.989
	0.236	0.371	1.657
	0.346	0.501	1.057
	0.227	0.605	0.868
	0.514	0.429	1.489
	0.179	0.303	0.985
	0.430		1.153
	0.216		0.655
			1.327
			0.785
			0.993
			0.350
			1.164
			0.526
			0.872
n	12	10	19
Average s_1	0.30	0.47	1.03

APPENDIX F

Values of Parameters k_1C and k_2C from Parallel Adsorption Model using Non-linear Regression

The parameters k_1C and k_2C directly estimated by non-linear regression analysis of the experimental data fit to the parallel adsorption model are given for each protein-surface contact in Table 11.

Table 11. Average values of k_1C and k_2C for each protein-surface contact from parallel adsorption model using non-linear regression.

Protein	Run #	Hydrophobic		Hydrophilic	
		$k_1C \times 10^3$	$k_2C \times 10^3$	$k_1C \times 10^3$	$k_2C \times 10^3$
Ile3→Cys (S-S)	1 2 3 4	7.20 5.50 3.90 4.70	7.60 6.20 6.00 5.40	3.10 6.30 6.00	4.30 9.00 13.3
Average		5.33	6.30	6.13	9.17
Wild Type	1 2 3 4	6.90 11.6 8.00 6.20	8.40 18.3 11.4 14.8	11.6 23.4 30.9	13.0 47.7 52.1
Average		8.18	13.23	21.97	37.6
Ile3→Trp	1 2 3 4	5.60 7.80 7.30 9.90	22.3 20.8 11.9 15.0	8.10 9.50 6.90 4.40	59.4 15.4 12.2 8.40
Average		7.65	17.5	7.23	23.85

APPENDIX G

Values of Parameters k_1C and k_2C from Parallel Adsorption Model using Linear Regression

The parameters k_1C and k_2C directly estimated by linear regression analysis of the experimental data fit to the parallel adsorption model are given for each protein-surface contact in Table 12.

Table 12. Average values of k_1C and k_2C for each protein-surface contact from parallel adsorption model using linear regression.

Protein	Run #	Hydrophobic		Hydrophilic	
		$k_1C \times 10^4$	$k_2C \times 10^4$	$k_1C \times 10^4$	$k_2C \times 10^4$
Ile3→Cys (S-S)	1	4.12	2.45	7.23	2.93
	2	2.91	2.71	2.34	2.60
	3	4.46	2.86	2.06	2.91
	4	5.04	3.06		
Average		4.13	2.77	3.88	2.81
Wild Type	1	3.26	2.99	1.68	1.99
	2	1.74	1.66	1.80	1.63
	3	3.94	1.73	2.57	1.99
	4	3.19	2.35		
Average		3.03	2.18	2.02	1.87
Ile3→Trp	1	0.25	1.87	0.28	2.20
	2	1.73	3.19	0.17	3.36
	3	1.14	3.58	1.42	2.25
Average		1.04	2.88	0.62	2.60

APPENDIX H

Raw Data of all Experiments

r_1 and r_2 are the most essential features of the adsorption kinetics (Appendix C). All raw data used in the calculation of r_1 and r_2, and other information pertaining to this research are kept in diskettes with Dr. Joseph McGuire in Department of Bioresource Engineering, Gilmore Hall, Oregon State University, Corvallis, OR 97331.